RTD-TDR-63-4106

RADIATION ACTIVATION OF PARA-ORTHO HYDROGEN CATALYSTS

TECHNICAL DOCUMENTARY REPORT NO. RTD-TDR-63-4106

DECEMBER 1963

AF Aero-Propulsion Laboratory
Research and Technology Division
Air Force Systems Command
Wright-Patterson Air Force Base, Ohio

Project No. 62-6199-3048, Task No. 304802

(Prepared under Contract No. AF 33(657)-8878 by Arthur D. Little, Inc., Cambridge, Massachusetts; Amos J. Leffler, Author)

NOTICES

When Government drawings, specifications, or other data are used for any purpose other than in connection with a definitely related Government procurement operation, the United States Government thereby incurs no responsibility nor any obligation whatsoever; and the fact that the Government may have formulated, furnished, or in any way supplied the said drawings, specifications, or other data, is not to be regarded by implication or otherwise as in any manner licensing the holder or any other person or corporation, or conveying any rights or permission to manufacture, use, or sell any patented invention that may in any way be related thereto.

Qualified requesters may obtain copies of this report from the Defense Documentation Center (DDC), (formerly ASTIA), Cameron Station, Bldg. 5, 5010 Duke Street, Alexandria 4, Virginia

This report has been released to the Office of Technical Services, U.S. Department of Commerce, Washington 25, D.C., for sale to the general public.

Copies of this report should not be returned to the Aeronautical Systems Division unless return is required by security considerations, contractual obligations, or notice on a specific document.

FOREWORD

This report was prepared by Arthur D. Little, Inc., Cambridge, Massachusetts, on Air Force Contract No. AF 33(657)-8878 under Task No. 304802 "Unconventional Fuels" of Project No. 3048, "Aviation Fuels." The contract efforts were accomplished under the cognizance of the AF Aero-Propulsion Laboratory, Research and Technology Division, Wright-Patterson Air Force Base, Ohio. The technical work was directed by Mr. P. R. Pitts as project engineer.

The investigation was carried out as C-64814 by Arthur D. Little, Inc. The author wishes to thank Mr. Bruce Ostar for his great help in the design, construction, and use of the catalyst measuring equipment. Thanks are also given to the staff of Arthur D. Little, Inc., for helpful discussions.

ABSTRACT

An investigation was carried out to determine whether improved catalysts for the para-ortho hydrogen conversion could be obtained by radiation. In the course of this work a series of catalysts were found that were as high as ten times more effective than a standard hydrated iron oxide catalyst at -78°C. Included in this series of catalysts were two that were radiation activated. As a result of this work an improved understanding of the catalytic mechanism was obtained.

This technical documentary report has been reviewed and is approved.

Marc P. Dunnam

Marc P. Dunnam

Chief, Technical Support Division

AF Aero-Propulsion Laboratory

TABLE OF CONTENTS

LIST OF TABLES

LIST OF TABLES (Continued)

LIST OF FIGURES

I. INTRODUCTION

This report describes the work carried out during the past year in an investigation designed to determine whether catalysts for para-ortho hydrogen conversion can be improved by radiation. The concept is based on interesting results that have been obtained in recent years from investigations into the effect of radiation on catalysts used in other reactions.

The initial work was carried out on commercial catalysts but no improvement due to radiation was found. Therefore, attention was shifted to materials specially prepared for this work and which were usefully affected by radiation. This has led to a series of new catalysts of high activity, among which are two that are affected by radiation, and to a more basic theoretical understanding of para-ortho hydrogen conversion.

Manuscript released by author August 1963 for publication as an RTD Technical Documentary Report.

II. DISCUSSION

The theory of the magnetically induced para-ortho hydrogen transition was developed by Wigner[1] and defined by Kalckar and Teller.[2] The theory, based on quantum mechanics, describes the conditions under which the hydrogen molecule can accomplish the strictly forbidden transition between an odd and an even nuclear spin state. Ortho-hydrogen has spins of 1, 3, 5---while para-hydrogen has spins of 0, 2, 4---. At low temperatures, equilibrium favors almost all of the hydrogen being in the para form with a nuclear spin of 0; at room temperature and above, the distribution is 75% ortho and 25% para. The probability of transition due to magnetic field is found to be:

$$W = \frac{8\mu_A^2 \mu_P^2 I\pi^2}{3h^8 a_s^6 kT} e^{-E_1/kT} \qquad (1)$$

where μ_A = magnetic moment of the proton

μ_P = magnetic moment of the paramagnetic ion

I = moment of inertia of the hydrogen molecule

a_s = distance of closest approach to the paramagnetic ion

and E_1 = energy difference between states

In this derivation it is assumed that the hydrogen molecule is brought with infinite velocity to the distance of closest approach, allowed to remain for the duration of the collision, and withdrawn, again with infinite velocity. It is quite obvious that such a process does not correspond to reality. Physically the process corresponds to a hydrogen molecule being adsorbed on the surface of a catalyst near a paramagnetic ion, being converted to the equilibrium state at that particular temperature, and then desorbing. This can be written as follows:

$$p\text{-}H_2\ (g) \rightleftharpoons p\text{-}H_2\ (ads) \qquad (2)$$

$$p\text{-}H_2\ (ads) \rightleftharpoons o\text{-}H_2\ (ads) \qquad (3)$$

$$o\text{-}H_2\ (ads) \rightleftharpoons o\text{-}H_2\ (g) \qquad (4)$$

In addition steps (2) and (4) are much more complex than is indicated here. Reactions can occur either on the surface or in the pores of a catalyst, and, therefore, each of these steps can be divided into two substeps: (1) the mass transfer of material from the gas stream to the surface of the catalyst and (2) diffusion into and out of the pores of the catalyst. In the following discussion each of the aspects of the catalytic process will be treated.

A. CONVERSION PROCESS

As was pointed out above, the conversion takes place when a hydrogen molecule is adsorbed on the surface of a catalyst near a paramagnetic ion. This implies two requirements: (1) a strongly inhomogeneous magnetic field and (2) a satisfactory surface for adsorption. The transition and rare earth ions are the most usual source of paramagnetic ions, although species such as O_2 and NO are also paramagnetic and have been shown to catalyze the para-ortho hydrogen transition. It should be realized that at low temperatures, paramagnetic species frequently show cooperative phenomena which renders them unsuitable as catalysts. These phenomena may include ferromagnetism, antiferromagnetism, or ferrimagnetism. The first is most commonly exhibited by metals such as Fe, Ni, and Gd below their Curie temperature and results when all the electron spins of the atoms are parallel in each domain.

Antiferromagnetism occurs when the spins of the metal ions align themselves in two sub-lattices with opposed spins. The sub-lattices may consist of the body-centered and corner ions respectively in a rutile lattice as in MnF_2, or in parallel planes as in MnO. The mechanism of exchange between two opposing spins occurs when the intervening anion donates an electron to one of the unfilled orbitals of the metal. This leaves the anion with a net spin antiparallel to that of the removed electron and the anion is thus coupled to the next adjacent metal ion. Many antiferromagnetic materials have been studied. Table 1 lists the Curie temperatures (below which antiferromagnetism occurs) for some of these materials. It can be seen that Fe_2O_3 is antiferromagnetic well above ambient temperatures, and this explains why hydrated iron oxide becomes ineffective as a catalyst when overheated during activation. It also suggests that FeO would be useful down to about 200°K and then would become ineffective and that Cr_2O_3 would be useful only above room temperature.

The values for the Curie temperatures in Table 1 apply only to the pure oxides. Dilution with non-paramagnetic materials will reduce the Curie temperature and make these materials paramagnetic at lower temperatures. Little data is available on this effect, but it is known that dilution greatly reduces interaction.

TABLE 1

CURIE TEMPERATURES FOR ANTIFERROMAGNETICS

Compound	Tc (°K)
MnF_2	72
FeF_2	79
MnO_2	84
MnO	122
FeO	198
Fe_2O_3	948
CoO	292
Cr_2O_3	328

Ferrimagnetism in non-conductors occurs when two non-equivalent sub-lattices exist but have a non-zero resultant force. These similarly have a temperature above which this interaction breaks down (Neel temperature). Examples of this class of materials are spinels, garnets, various fluorides such as $Na_5Fe_3F_{14}$, and certain metal sulfides such as Fe_7S. Because of the complexity of their preparation and their lack of apparent advantage over other compounds, no work has been done with these materials as ortho-para hydrogen catalysts.

A ferromagnetic or ferrimagnetic substance may function as a catalyst if it is finely enough divided on a diamagnetic surface. Each clump of ferromagnetic atoms is a single magnetic domain, and if these domains are randomly oriented, the entire assembly acts as a paramagnetic substance. This phenomenon, called "superparamagnetism,"[3] is typified by reduced nickel on silica. The effectiveness of these domains for para-ortho hydrogen catalysis is probably less than the sum of the single atom, since the effectiveness of a material depends on the field gradient acting on a hydrogen molecule. The field gradient is the same for a large particle as for a single ion, but molecules of hydrogen approaching the large particle at a constant velocity see a smaller gradient than for a small ion.

B. DIFFUSION

As was pointed out above, a critical factor affecting the efficiency of a heterogeneous catalyst is the rate at which the reactants are brought to the active sites of the catalyst. This is a two-step process; (1) the mass transfer of material from the gas stream to the surface of the catalyst and (2) diffusion into and out of the pores of the catalyst. Diffusional problems are basic to chemical engineering and have been extensively treated in standard works.[9]

In heterogeneous reactions, the rate-controlling step at flow rates of interest is usually pore diffusion. However, at relatively low flows, longitudinal diffusion along the path length can be significant. This problem has been recently treated[10] in an elegant manner for the high-temperature dissociative mechanism of para-ortho hydrogen conversion. It was shown that a criterion exists to determine whether longitudinal diffusion is an important factor. This criterion is the ratio:

$$\psi = \frac{D_{eff} k}{V^2} \geq 1 \qquad (5)$$

where D_{eff} = effective diffusivity in the bed

k = rate constant defined as $k = \frac{1}{t} \ln\left(\frac{y_{eq} - y_i}{y_{eq} - y_i}\right) \times \frac{T_{Reactor}}{T_{Ambient}}$

V = linear gas velocity

t = residence time in the bed

This criterion was employed to analyze the data obtained in the present work. In a typical high efficiency catalyst it was found that only at the very low flow rates was the value of ψ greater than 1. In these calculations the value of D_{eff} used was that experimentally determined as will be described below. This value is in the order of 0.005 cm^2/sec, which is much less than the gaseous self-diffusion constant of hydrogen of 1.2 cm^2/sec employed by the original workers in their calculations. The difference was due to the fact that in the present work the reactor was a bed of particles; the original workers used platinum gauze. In the present apparatus, with a bed diameter of 1.0 cm and length of approximately 0.5 cm, ψ was greater than 1 for flow rates of 120 cc/min or less; thus, at the high flow rates used in this work, longitudinal diffusion is unimportant.

At high flow rates, the rate-controlling factor is pore diffusion in the catalyst particles. In the present work, we measured the bulk density, surface area, and pore volumes for some of the catalysts under investigation and used this data to calculate the effective diffusion coefficient, D_{eff}, by the method of Weisz and Schwartz.[11] The relation used is:

$$D_{eff} = \frac{2.14 \times 10^{5} d_{Hg}^{2} P_{v}^{3}}{S} \qquad (6)$$

where d_{Hg} = bulk density of the catalyst

P_v = pore volume of the catalyst

and S = surface area of the catalyst

The results are given in Table 2.

TABLE 2

EFFECTIVE DIFFUSIVITIES OF ACTIVE CATALYSTS AT 298°K

Catalyst	D_{eff} in $\frac{cm^2}{sec}$
AP-1	0.0204
AP-1 Soaked in Boric Acid	0.0160
No. 38	0.0353

The values are in general agreement with values obtained for catalysts of similar structure.

A comparison of the values of D_{eff} measured for the catalysts listed in Table 2 and the values of D_{H_2} all calculated at a temperature of 195°K are given in Table 3. The correction to 195°K for D_{eff} was made by assuming that the D_{eff} values are for Knudsen flow and the relation:

$$D_{K.eff}^{(T)} = \sqrt{\frac{T}{298}}\, D_{K.eff}^{(298)} \quad \text{holds} \qquad (7)$$

TABLE 3

EFFECTIVE DIFFUSIVITIES OF ACTIVE CATALYSTS AT 195°K

Catalyst	$D_{K.eff}$ in $\frac{cm^2}{sec}$
AP-1	0.0165
AP-1 Soaked in Boric Acid	0.0130
No. 38	0.0284
Gaseous Hydrogen at 30 atm. Pressure	0.0224

A calculation was made for the mean free path of hydrogen at 195°K and 30 atmospheres pressure and it was found to be 20.6 Å. This indicates that the flow through the catalyst is going to be a combination of Knudsen flow and bulk diffusion. The bulk diffusion coefficient is calculated from the relation:

$$D_{H_2\,eff} = \frac{D_{H_2}\,\theta}{\tau} \qquad (8)$$

where θ is the void fraction and τ the tortuosity. The value of θ is that of the pore volume which has already been determined and τ has a value of about 2 in most cases. The composite diffusion coefficient is calculated from the Knudsen and bulk coefficients.

$$\frac{1}{D_{eff}} = \frac{1}{D_{Keff}} + \frac{1}{D_{H_2\,eff}} \qquad (9)$$

Values of $D_{H_2\,eff}$ and D_{eff} are given in Table 4.

TABLE 4

VALUES OF D_{H_2} AND D_{eff} FOR ACTIVE CATALYSTS AT 195°K

Catalyst	$D_{H_2\,eff}$ in $\frac{cm^2}{sec}$	D_{eff} in $\frac{cm^2}{sec}$
AP-1	0.00865	0.00606
AP-1 Soaked in Boric Acid	0.00788	0.00491
No. 38	0.00560	0.00467

At 77°K for AP-1, D_{Keff} is 0.0114 cm^2/sec and D_{H_2} is 0.0224 cm^2/sec at 100 psig. The value of $D_{H_2\,eff}$ is 0.00865 cm^2/sec giving a value of D_{eff} of 0.00624 cm^2/sec. This latter value was used to calculate h tanh h and E in Table 6.

When the effective diffusivity of a catalyst is known, it is possible to calculate the effective use of the active sites of the catalyst. The number and accessibility of these sites are criteria of effective use, which will vary with the flow rate and conditions. The effective use of a catalyst is defined by the effectiveness factor:

$$E = \frac{\tanh h}{h} \tag{10}$$

where

$$h = \left[\frac{2k}{r\,D_{eff}}\right]^{\frac{1}{2}} \tag{11}$$

and k is the first order rate constant per unit of surface area and r is the average pore radius.

Wheeler has derived a more useful expression to calculate h:

$$h \tanh h = \left(\frac{a^2}{18D_{eff}}\right)\left(\frac{F.R.}{C_A(\text{Inlet})}\right)\left(\frac{1}{P_v d_{Hg}}\right) \ln\left(\frac{y_{eq} - y_i}{y_{eq} - y_o}\right) \tag{12}$$

where a = catalyst particle diameter

$F.R.$ = feed rate to the reactor

$C_A(\text{Inlet})$ = inlet concentration of the reactant

and $\dfrac{y_{eq} - y_i}{y_{eq} - y_o}$ = reciprocal of the fraction converted

At values of h much above 1, tanh h approaches 1 and the expression gives the value for h. Then E is simply the reciprocal of h.

Based on our experimental data we have evaluated the value of h tanh h for a number of different catalysts. The data are given below in Tables 5 to 7 and represent the highly efficient Air-Products catalyst (AP-1) at two temperatures and a high efficiency catalyst developed in the present work.

TABLE 5

VALUES OF EFFECTIVENESS FACTOR OF AP-1 AT -78°C AND 500 PSIG

Flow Rate in cc/min/gm cat.	h tanh h	E
7,920	10.67	0.094
14,500	13.40	0.0746
22,130	15.38	0.0650

TABLE 6

VALUES OF EFFECTIVENESS FACTOR OF AP-1 AT -195°C AND 100 PSIG

Flow Rate in cc/min/gm cat.	h tanh h	E
4,530	24.28	0.0412
6,100	29.88	0.0335
8,000	34.68	0.0288
9,900	38.41	0.0260
12,200	42.17	0.0237
14,300	45.14	0.0222
17,700	49.10	0.0204

Calculated from Air Product Co. data 1/8" bed.

TABLE 7

VALUES OF EFFECTIVENESS FACTOR OF NO. 38 AT -78°C AND 500 PSIG

Flow Rate in cc/min/gm cat.	h tanh h	E
2,600	504.2	0.00198
5,830	768.7	0.00130
15,650	1188.2	0.00084

A comparison of Tables 5 and 7 shows that the AP-1 catalyst utilizes a much larger fraction of its effective sites than does No. 38. This is certainly due in part to the difference in particle size, since h is directly proportional to the square of the diameter of the particles and E is inversely proportional to h. The difference is probably not as great as indicated, since in the present equipment the catalyst particles are crushed in opening the capsule.

An effective use of the catalyst sites is desirable in order to make the catalyst less sensitive to poisoning. If the number of active catalyst sites is very small, a small amount of impurity will effectively inactivate the catalyst. A very recent study[12] has been made on this subject and it has been shown that AP-1 can be inactivated by an impurity of 60 ppm of nitrogen in the hydrogen. This very low level indicates the great sensitivity of para-ortho hydrogen catalysts to poisoning. It also casts considerable doubt on much of the data in the literature because the care taken to purify the hydrogen used was probably not great enough to reduce the impurity level below that which would seriously affect the catalyst. This was found to be the case in the present work in some initial measurements where the activity of some of the more active catalysts were found to be much lower than expected at 77°K. Most of the measurements were made at 195°K (-78°C) where the adsorption of nitrogen is not a problem, and, therefore, the activities would be much less likely to be affected by the impurities normally present in hydrogen.

The fact that D_{eff} of the catalysts are within an order of magnitude of the D_{H_2} indicates that at low flow rates of gas there will be an insufficient amount of unreacted para hydrogen at the surface of the catalyst. Therefore, the plot of log $\left(\frac{y_{eq} - y_i}{y_{eq} - y_o}\right)$ vs $\frac{W}{F}$ will show a deviation from a straight line since mass transfer to the catalyst particle surface is a factor. This deviation is observed with all of the more active catalysts.

C. PRESSURE DEPENDENCE

The present work confirmed previous findings that the rate of conversion is pressure dependent. In the present work, the tests were run at 100, 300, and 500 psig of hydrogen pressure and the rate constants were always lower at 100 pounds pressure but showed little difference at the higher pressure. This can be explained by the Langmuir-Hinshelwood hypothesis[13] that adsorption is the controlling mechanism. This hypothesis states that the equilibrium is essentially undisturbed by the reaction* and that the fraction of surface covered is related to the pressure of the relation:

$$\theta = \frac{Kp}{1 + Kp} \tag{13}$$

where K is the equilibrium constant and p is the pressure.
The rate of reaction is proportional to θ:

$$v = \frac{k_a Kp}{1 + Kp} \tag{14}$$

where k_a is the rate constant.

It can be seen that if Kp is large with respect to 1, then the expression reduces to: $v = k_a$, i.e., independent of pressure, and if Kp is small with respect to 1, then the expression becomes:

$$v = k_a Kp \tag{15}$$

In the present work at the higher hydrogen pressures, $Kp >> 1$; therefore, the rate is pressure independent.

D. EFFECT OF RADIATION ON CONVERSION PROCESS

The effect of radiation on solids has been extensively investigated and has been summarized in a number of reviews.[4,5] For the purposes of the present work the most important effects of radiation are those that affect the paramagnetism of the catalyst. This can occur by a number of different mechanisms as discussed below.

---

*It has been shown that the heat of vaporization for o-hydrogen is 4.3 cal/mole higher than for p-hydrogen.

For the purpose of this work, the most important effect of radiation on solids is the production of paramagnetic units such as F centers. These are electrons trapped in vacant anionic lattice sites. A recently published report[6] describes irradiation of magnesium oxide with Co^{60}; measurements of catalytic activity of this material showed that irradiation enhanced the catalytic activity by factors of 2 to 3. In the present work, it was found that alumina was considerably activated by X-ray treatment, although this may have been due to the presence of trace amounts of metal impurities.

A second effect of X-ray radiation is the reduction of metal ions to lower valency states. This has been reported to occur for V^{3+} in alumina.[7] Presumably V^{2+} in a high enough concentration should be a more effective catalyst than V^{3+}, since the latter is not paramagnetic while the former has one unpaired electron.

Finally, radiation affects physical structure. Such an effect occurs chiefly in the case of heavy particle treatment, such as fast neutron or alpha bombardment. Here, there is general lattice disruption, which presumably increases surface area and allows hydrogen molecules better access to the catalytic centers. As a result, an irradiated sample shows greater activity than untreated material. It must be pointed out, however, that irradiation in a nuclear reactor is a complex process; since all types of particles are present, it is difficult to be certain that a particular effect is due to one type of radiation rather than a combination of effects.

Given below in Tables 8 to 14 are the results of various treatments on a number of different catalyst systems. Unfortunately, it is not permitted to discuss the results in detail here, since the composition of a number of the more interesting systems has been classified.

One important aspect is the variability of the results. Both in catalysis work and in radiation work variable results are common. The variability encountered in this study, which combined work in both areas, is especially evident in the experiment reported in Table 10, where an originally inactive sample became extremely active after treatment with 300 KV X rays with an intensity of 90,000 rads/hr. Another group of samples were treated with Co^{60}, which has 1.28 and 1.17 mev gamma rays. This was carried out at the U.S. Army Quartermaster Laboratory, Natick, Mass., where the radiation intensity is 3.11 megarads/hr. It is quite evident that further study is needed to determine what conditions will yield the most active catalyst.

It was also noted that there was a considerable loss in catalytic activity over a period of 24 hours during which the catalyst was allowed to remain in contact with the hydrogen. The cause of this loss in activity was not investigated but may be due to impurities in the hydrogen covering the active sites or perhaps to migration of the active sites into the lattice out of contact with the hydrogen.

No attempt was made to determine whether the period of time elapsing after radiation had any effect on catalyst activity, although during this period the catalyst remained in the evacuated sealed ampoule. The time between irradiation and testing varied from several days to about two weeks. It is evident that this effect should also be investigated.

TABLE 8

EFFECT OF VARIOUS TREATMENTS OF C. K. WILLIAMS IRON OXIDE CATALYST*

Sample No.	Treatment	K_{ov500} $\frac{\text{gm mole } H_2}{(\text{gm of catalyst})(\text{min})}$ at -78°C
35	Original	0.0718
43	Irradiated in Hydrogen 92.53 hr	0.0575
55	Soaked in Saturated Boric Acid	0.0207
47	Soaked in Saturated Boric Acid Two Minutes in Nuclear Reactor	Inactive
51	Soaked in Saturated Boric Acid One Hour in Nuclear Reactor	0.0502

*All samples were activated by heating to 130°C at 10^{-6} mm Hg for 16 hours.

TABLE 9

EFFECT OF VARIOUS TREATMENTS OF AP-1* CATALYST

Sample No.	Treatment	K_{ov500} $\frac{\text{gm mole } H_2}{(\text{gm of catalyst})(\text{min})}$ at -78°C
34	Original	0.346
29	Irradiated 63.94 hr	0.345
46	Irradiated Under Hydrogen 92.53 hr	0.138
54**	Soaked in Saturated Boric Acid	0.487
57	Repeat of 54	0.622
48	Soaked in Saturated Boric Acid Two Minutes in Nuclear Reactor	0.344
50	Soaked in Saturated Boric Acid One Hour in Nuclear Reactor	0.098

*All samples were activated by heating to 285°C at 10^{-6} mm Hg for 16 hours.

**There was some hydrogen leakage in the equipment in Sample 54 and a repeat (No. 57) was run.

TABLE 10

EFFECT OF VARIOUS TREATMENTS ON SAMPLE NO. 38*

Sample No.	Treatment	K_{ov500} $\frac{\text{gm mole } H_2}{(\text{gm of catalyst})(\text{min})}$ at -78°C
38	Original	0.391
39	Irradiated 5.75 megarads	0.218
56	Soaked in Saturated Boric Acid	Inactive
52	Soaked in Saturated Boric Acid One Hour in Nuclear Reactor	0.0655
79	Soaked Initially in Saturated Boric Acid	0.260
61	Soaked Initially in Saturated Boric Acid Irradiated 6.77 megarads	0.115
66	Soaked Initially in Saturated Boric Acid Irradiated 10 Hours in Nuclear Reactor	0.23

*All samples were activated by heating to 400°C at 10^{-6} Torr for 16 hours.

TABLE 11

EFFECT OF VARIOUS TREATMENTS ON SAMPLE NO. 40*

Sample No.	Treatment	K_{ov500} $\frac{\text{gm mole } H_2}{(\text{gm of catalyst})(\text{min})}$ at -78°C
40	Original	Inactive
41	Irradiated 2.8 megarads	0.161
53	Soaked in Saturated Boric Acid One Hour in Nuclear Reactor	0.0577
63	Soaked Initially in Saturated Boric Acid	0.173
64	Soaked Initially in Saturated Boric Acid Irradiated 6.77 megarads	0.218
67	Soaked Initially in Boric Acid 10 Hours in Nuclear Reactor	0.242

*Samples were activated by heating to 400°C at 10^{-6} Torr for 16 hours.

TABLE 12

EFFECT OF X RAY AND Co^{60} IRRADIATION ON SAMPLE NO. 59*

Sample No.	Treatment	K_{ov500} $\frac{\text{gm mole } H_2}{(\text{gm of catalyst})(\text{min})}$ at -78°C
59	Original	Inactive
60**	Irradiated 7.35 megarads	0.391
68**	Irradiated 11.0 megarads	0.541
	After 24 hours	0.208
75R**	Irradiated 7.62 megarads	0.115
76**	Irradiated 12.00 megarads	0.276
77**	Irradiated 18.00 megarads	0.184

*Samples were activated by heating to 400°C at 10^{-6} Torr for 16 hours.

**Nos. 60, 68 were irradiated in 300 KV X-ray source; Nos. 75R, 76, 77 were irradiated in Co^{60} source.

TABLE 13

EFFECT OF VARIOUS TREATMENTS ON SAMPLE NO. 69*

Sample No.	Treatment	K_{ov500} $\frac{\text{gm mole } H_2}{(\text{gm of catalyst})(\text{min})}$ at -78°C
69	Original	0.368
70	Irradiated 97.56 hours	Inactive
71	Soaked in Saturated Boric Acid	Inactive
78	Soaked in Saturated Boric Acid 10 Hours in Nuclear Reactor	0.760

*Samples were activated by heating to 400°C at 10^{-6} Torr for 16 hours.

TABLE 14

EFFECT OF X-RAY IRRADIATION ON SAMPLE NO. 72*

Sample No.	Treatment	K_{ov500} $\frac{\text{gm mole } H_2}{(\text{gm of catalyst})(\text{min})}$ at -78°C
72	Original	0.345
73	Irradiated	0.205
86	Soaked in Saturated Boric Acid	0.138
89	Soaked in Saturated Boric Acid 10 Hours in Nuclear Reactor	0.047

*Samples were activated by heating to 400°C at 10^{-6} Torr for 16 hours.

E. MISCELLANEOUS CATALYSTS

In addition to the radiation studies discussed above, a number of other catalysts were investigated. These included a series of metal ions deposited on silica gel as shown in Table 15. It can be seen that the catalysts were very inactive and that radiation had little effect on their activity. Because of this low activity, no further work was carried out on these systems.

In addition to the above materials, a few other possible catalysts were investigated. These are listed in Table 16. The cyclopentadienyls were tried because they are known to have unpaired electrons and hence should be catalytic. It appears that the geometric structure of the molecules does not allow the hydrogen molecules to approach close enough to the central atom to be affected. The iridium carbonyl compound was studied, since recent reports in the literature[8] indicated that hydrogen is reversibly absorbed by this molecule. This would allow spin equilibration to take place, and if the absorption were rapid enough, the compounds would be effective catalysts. It appeared that, at the low temperatures used in this work, the hydrogen was irreversibly absorbed destroying the catalytic activity of the compound. A less active compound would be interesting, but this would necessitate a synthesis program that could not be justified.

TABLE 15

EFFECTIVENESS OF METAL OXIDES DEPOSITED ON SILICA GEL
(conversion at 85 ml/min at 100)

Catalyst	Analysis	Unirradiated Wt (gm)	Unirradiated % Para	Irradiated Wt (gm)	Irradiated % Para	Irradiation Dosage
Silica Gel*			50.26			
Cr_2O_3	144%	0.4051	45.60			
NiO	0.8	0.3794	47.85	0.3394	45.45	5.87 megarads
Al_2O_3	3.05	0.4105	35.39			
Fe_2O_3	0.99	0.3764	46.87	0.3348	42.85	11.6 megarads
Fe_2O_3	2.15	0.2468	45.35	0.3443	44.91	5.87 megarads
Fe_2O_3	4.20	0.3271	44.11			
NiO	0.82	0.3779	49.00	0.3573	46.26	11.6 megarads
CuO	1.84	0.3583	44.70			
Pyrex					50.26 (no conversion)	

*Not well crushed

TABLE 16

MISCELLANEOUS CATALYSTS

Sample No.	Description	K_{ov500} $\frac{\text{gm mole } H_2}{(\text{gm of catalyst})(\text{min})}$ at -78°C
42	Alumina Irradiated 5.75 megarads	0.0327
49	Ru $(C_5H_5)_2$	Inactive
58	Ni $(C_5H_5)_2$	Inactive
74	Ir (CO) Cl $\left[(C_6H_5)_3\ P\right]_2$	Inactive

III. EXPERIMENTS

A. APPARATUS

1. Catalyst Activity Measuring Equipment

The apparatus used in this study is similar to apparatus described in the literature[14] for the study of para-ortho conversion. It does differ from some of the apparatus described in that it is necessary, since para to ortho kinetics are being studied, to prepare low-temperature equilibrated hydrogen. This was done in a high-pressure, stainless-steel vessel in which a cylinder of catalyst is placed along the center line. To ensure that equilibrium concentration would be reached in a reasonable time, the system model was set up as a diffusion-controlled reaction and solved for the geometry of the system. The results are shown in the Appendix.

A schematic diagram of the apparatus is shown in Figure 1. The apparatus is designed to run catalyst studies up to 600 psig or, with slight modification, up to 1000 psig. The hydrogen used for this work is General Dynamics' electrolytic grade material. The material is passed through a "Deoxo"unit to remove oxygen. Any water produced is removed in a silica gel drier. The hydrogen is then cooled to -196°C in the coil and passed through a silica gel column to remove any noncondensible gases other than helium. (Since this is electrolytic grade material, there should be no helium present.) The main portion of the hydrogen is then passed into the high-pressure storage vessel mentioned above for conversion to the equilibrium gas at either 77° or 65°K. During operation a small stream of hydrogen is taken from the silica gel trap at -196°C, warmed to ambient temperature, and passed through a commercial catalyst to convert it to normal material to be used as the reference gas in the thermal conductivity unit.

The hydrogen from the low-temperature storage tank is pressure-controlled by a Hoke pressure regulator and passed through the catalyst under test. Since most of the runs were made with the catalyst at -78°C, a 20' cooling coil was added to cool the hydrogen gas before it enters the catalyst chamber. This was shown to be adequate for all flow rates encountered in this work. (The hydrogen can bypass the catalyst if comparison with standard hydrogen is desired.) After passing through the catalyst, the hydrogen is passed through a stainless steel disc, then through a high-pressure rotameter and then through a pressure regulator, where it is dropped to atmospheric pressure. A small stream is taken off to be passed through the thermal conductivity cell for comparison with standard hydrogen; the remainder is passed to a wet test meter.

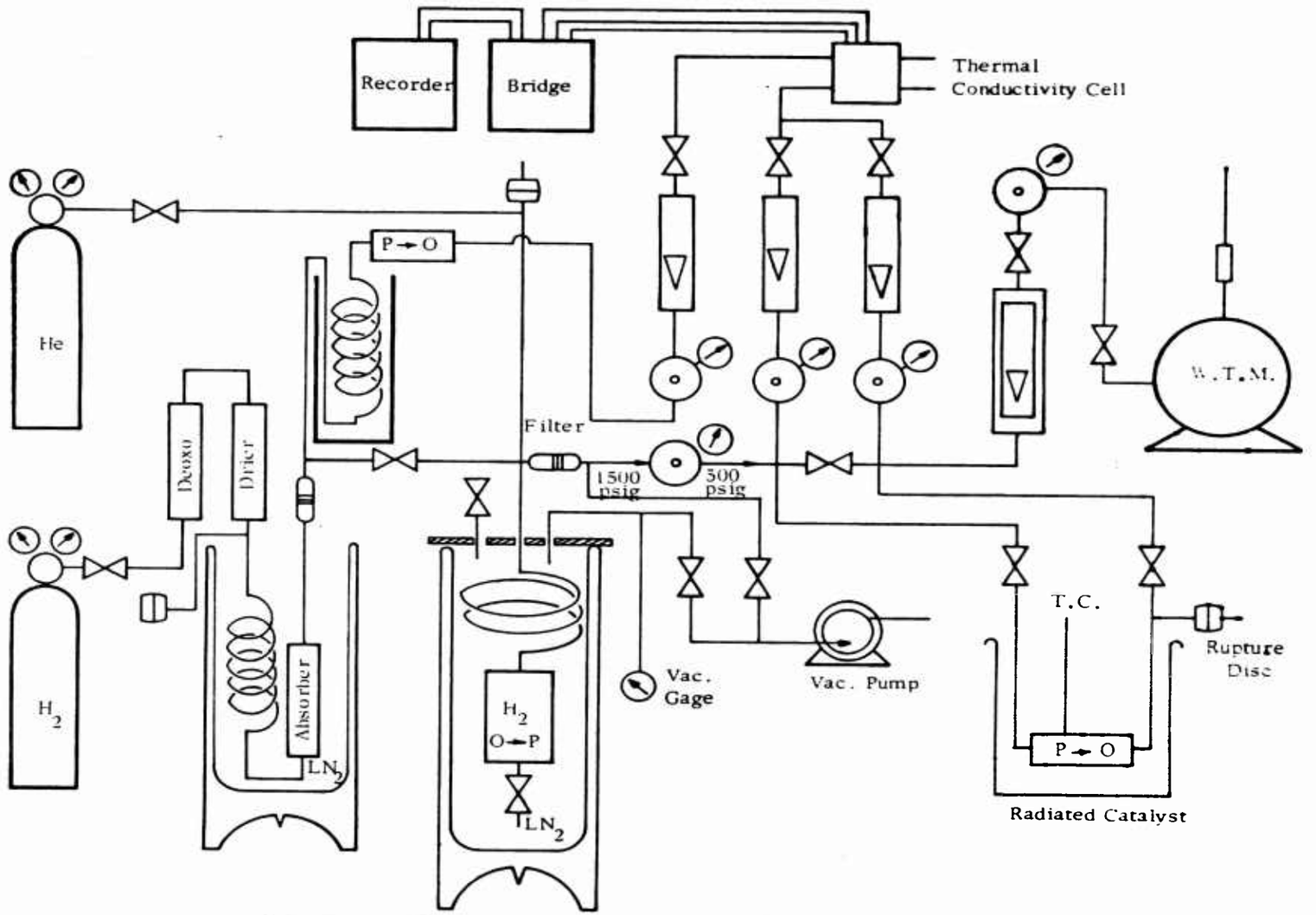

FIGURE 1 SCHEMATIC DIAGRAM OF CATALYST MEASURING EQUIPMENT

The measurement system consisted of a Gow-Mac 9677 conductivity bridge using thermistors. The bridge has more than ample sensitivity for the measurements. For the constant voltage source, a 12-volt storage battery was used. Small fluctuations in thermistor current were adjusted by a General Radio decade box. The conductivity cell was kept at 0°C in a Dewar flask. We have found that packing with wet ice each morning kept the cell at 0°C for a full day. The output of the cell was read on a Brown recorder. A Helipot across the bridge output was used to control full-scale voltage. Cell current was kept at 11.00 milliamperes, as read on a Weston precision miliammeter. Because of the high sensitivity of the cell, small changes in current cause appreciable changes in the output; current fluctuations, however, were adjusted with the decade box.

The hydrogen storage cylinder was kept at -196°C, but the temperature could be lowered by pumping to the triple point of nitrogen (-210°C), which would permit a 62% parahydrogen mixture to be studied in comparison with the normal gas (25% parahydrogen). Liquid hydrogen can be used as starting material if it is desired to work with essentially pure parahydrogen; however, pressures will be below the critical value of 188 psia and the present work specified high pressures.

In this work the catalyst must be irradiated in separate equipment and then placed in the system without any exposure to air. Therefore, a special reactor was designed. (See Figure 2.) The catalyst was activated, sealed in a glass capsule, and then irradiated either with X rays or neutrons. The capsule was placed in the crusher, which was then attached to the system, and flushed with hydrogen. The capsule was thoroughly crushed and measurements made. The crusher was equipped with stainless-steel sintered discs to prevent catalyst particles and glass from being carried around the system.

In addition to the conversion measuring system described above, we constructed a standard BET surface-area measuring system. The catalyst was activated by heating to a desired temperature under vacuum, the surface area measured, and then the catalyst sealed off for irradiation. In this way, the surface area of each catalyst used was known.

2. Measurement of Catalyst Density by Mercury Displacement

The equipment used is shown in Figure 3. It was constructed from a 10 ml pipette, which was altered by putting a coarse glass frit on the bottom with a standard taper below. A second standard taper, placed at the top of the tube, fitted into an addition device that permitted adding mercury to the evacuated system without the introduction of air.

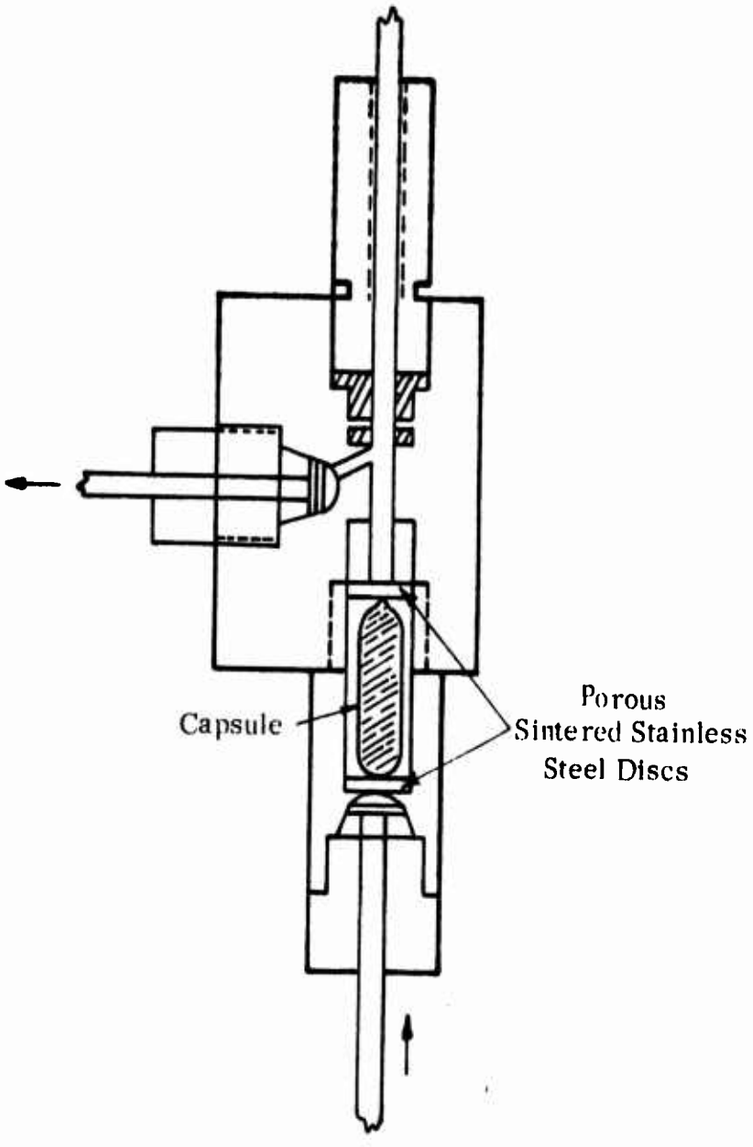

FIGURE 2 CRUSHER REACTOR FOR CATALYST CAPSULES

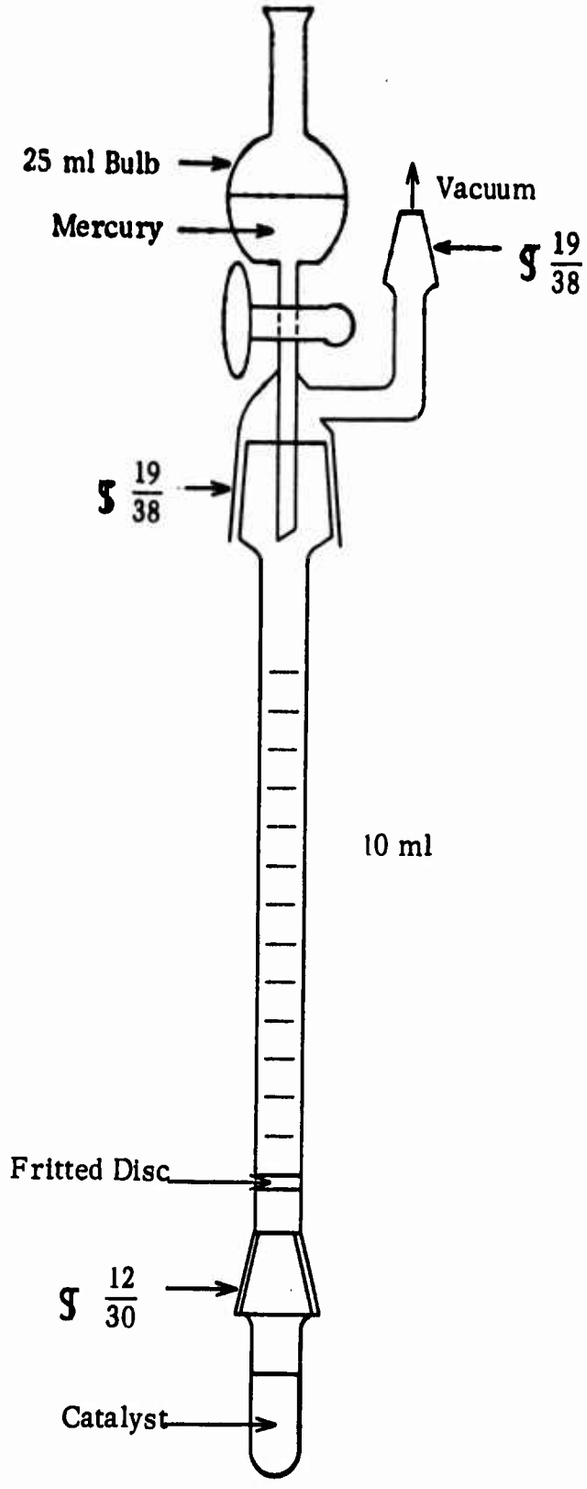

FIGURE 3 APPARATUS FOR MEASUREMENT OF CATALYST DENSITY BY MERCURY DISPLACEMENT

3. Measurement of Catalyst Density by Helium Displacement

The apparatus used was that described by Rossman and Smith[15] and shown in Figure 4. One change made in the equipment was the addition of a stopcock at B in order to prevent bubbling of gas through the mercury column when excess pressure was admitted to the system. The stopcock could be carefully opened and the excess pressure removed. This prevented mercury turbulence, which usually results in breakage of the system.

B. PROCEDURE

1. Catalyst Activity

The catalyst was weighed by difference in an 8-mm tube sealed at one end. The tube was then attached to the surface-area measuring system and the catalyst activated by heating and pumping under specified conditions. After the surface area was determined, the catalyst was sealed under vacuum in a capsule which fitted in the crusher.

The capsule was either placed in the crusher and opened immediately or irradiated by X rays or in the Massachusetts Institute of Technology Nuclear Reactor. Since there are specific size limitations for objects to be placed in the nuclear reactor, the dimensions of the capsule were chosen so that the capsule could be placed in an aluminum can for reactor irradiation. After irradiation, the capsule could be placed in the crusher and opened in the same way as the unirradiated control specimens. However, specimens irradiated in the nuclear reactor may have to stand for a period of time to permit the decay of short-lived nuclides. This is especially important in the case of catalysts containing iron and nickel, because of the formation of Fe^{59} and Ni^{65}, both of which decay with penetrating X rays and hence present a safety problem. It was found that after the initial radiation due to silicon disappeared, the catalysts were not too active to be handled with ordinary precautions.

After the capsule was placed in the crusher, the system was purged with hydrogen from the storage system. The capsule was then crushed by turning the handle. Various flow rates and pressures were set by adjustment of the pressure regulator and rotameter valves. The hydrogen flow through the catalyst was the sum of the flow through the conductivity cell and the flow through the wet test meter.

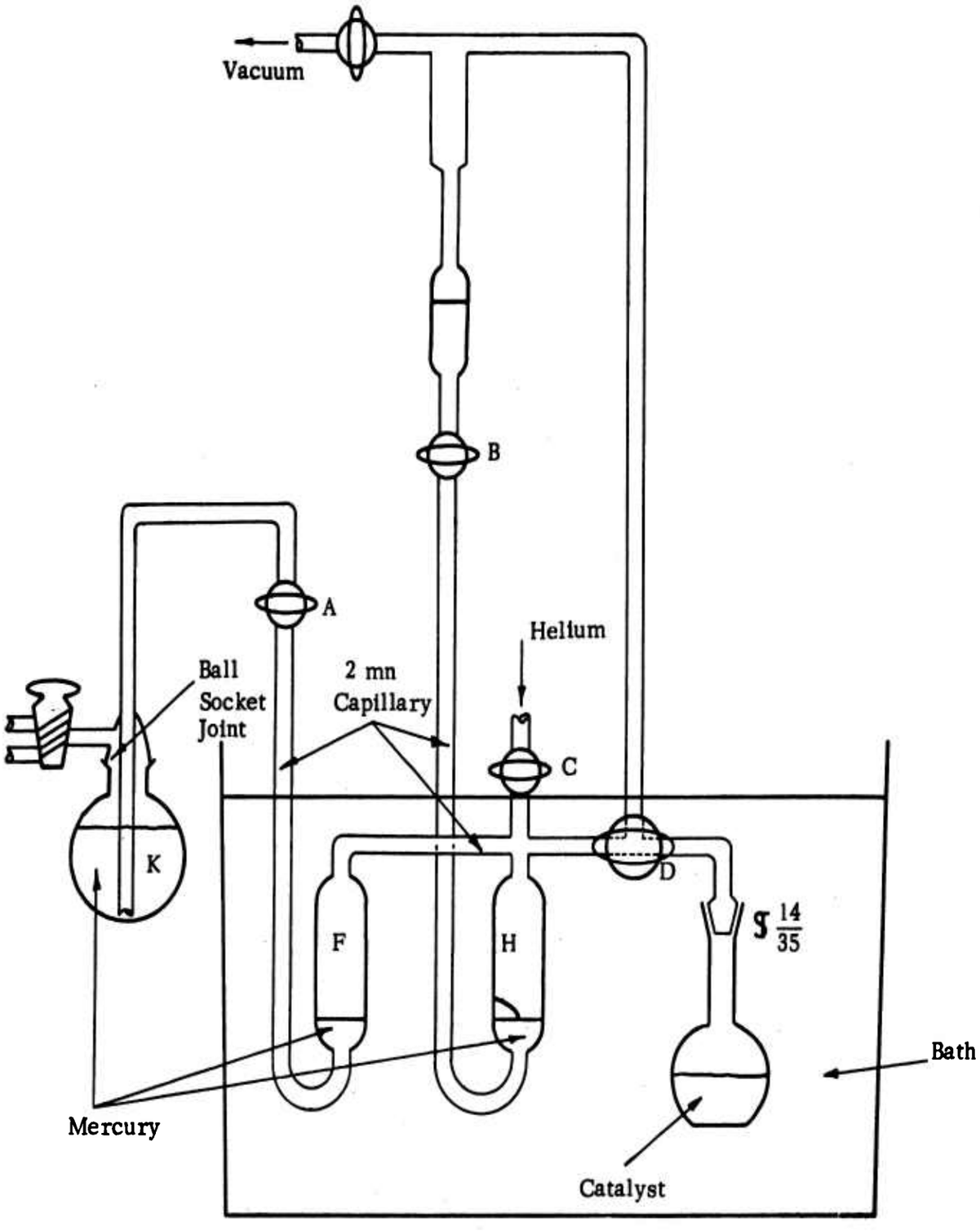

FIGURE 4 APPARATUS FOR MEASUREMENT OF CATALYST DENSITY BY HELIUM DISPLACEMENT

The voltage output of the thermal conductivity cell was shown on the recorder. It has been reported in the literature that changes of voltage are proportional to changes in the para-ortho content of the hydrogen. Therefore, once the voltage output of the normal and low-temperature equilibrium forms of the hydrogen were indicated on the recorder, the concentration of intermediate mixtures could be determined by proportionality relations.

2. Measurement of Catalyst Density by Mercury Displacement

A sample of catalyst was weighed into the small container by difference. Enough material was taken to fill about two-thirds of the volume. The standard taper was lightly greased, attached to the remainder of the apparatus, and the volume was then evacuated through the side arm. In the present work, the dried but unactivated catalyst was used, since it was not believed likely that there would be any large change in density during activation. After evacuation, mercury was carefully added to the system in an amount great enough to fill the space below the fritted disc.

The level of the mercury in the column was read, and air was admitted to the system to force the mercury through the fritted disc. When the volume below the disc was filled with mercury, the level was read in the column and the difference between the two readings was the amount of mercury needed to fill the volume. An initial calibration with the empty system gave the empty volume below the frit, and the difference between this value and that found for a given weight of sample gave the volume occupied by the sample. The weight of the sample divided by the volume so determined gave its bulk density.

3. Measurement of Catalyst Density by Helium Displacement

A weighed sample of catalyst was placed in the container as indicated. Since helium penetrates into the pores, it was felt necessary to activate the material at an elevated temperature. This was carried out on the vacuum system and the container filled with nitrogen and stoppered. It was then attached to the system, the bath raised, and the system evacuated with stopcock B closed. Stopcock B was carefully opened to determine whether the pressure was sufficient to support the mercury column with the lower level at the pointer. If the level was close to the pointer, C was closed and the final adjustment made by removing or adding mercury through A. When the level was properly adjusted, flask K was weighed. Stopcock D was then opened with B closed and helium allowed to expand into the catalyst vessel. Stockcock A was opened and mercury from K admitted to F, so as to readjust the mercury level back to the pointer with B open. The flask K was

then weighed, and the difference between the two weighings gave the volume of the catalyst vessel up to D at the bath temperature. An initial calibration of the catalyst vessel gave the empty volume, and the difference between the two volumes gave the volume of the catalyst. The weight of the catalyst divided by the volume gave the density of the catalyst.

C. CATALYST PREPARATION

The catalyst preparation of the more active materials is classified and may not be described here. The preparation of the oxides on silica gel is described below.

A commercial silica gel was obtained from the Davison Chemical Company. The gel was PA100-refrigeration grade and was found to have a surface area of 765 m^2/gram.

The following procedure was used to coat this material with various metal oxides for the purpose of testing the oxide as a catalyst.

500 ml of a 0.5 molar solution of the hydrated nitrate was placed in a crystallizing dish and to this was added 100 grams of the Davison gel. The mixture was stirred periodically to remove air bubbles and allowed to stand for 24 hours. The gel was then drained on a Buchner funnel over suction until thoroughly drained (about 20 minutes). The drained material was transferred to a clean dish and dried in a 100°C drying oven for 24 hours. The adsorbed nitrate was usually partly decomposed during the drying, and it was necessary to keep the oven in a hood to remove NO_2 fumes. The dry gel was transferred to a crucible and fired in a muffle furnace at 500°C for 24 hours. When cool, the gel was set aside for later use, and a small sample sent for analysis of the metal content.

In the irradiations carried out in the nuclear reactor, quartz capsules were used because the presence of boron in pyrex glass causes excessive heating.

D. RESULTS

1. Catalyst Activity

The procedure used for the calculations of the results was that described in reference (12). In our work, pressures of 500, 300 and 100 psig of hydrogen were used. Only the $I_{ov\,500}$ values are given in the Tables, but the values for 300 psig were very close to those for 500 psig, while those for 100 psig were lower.

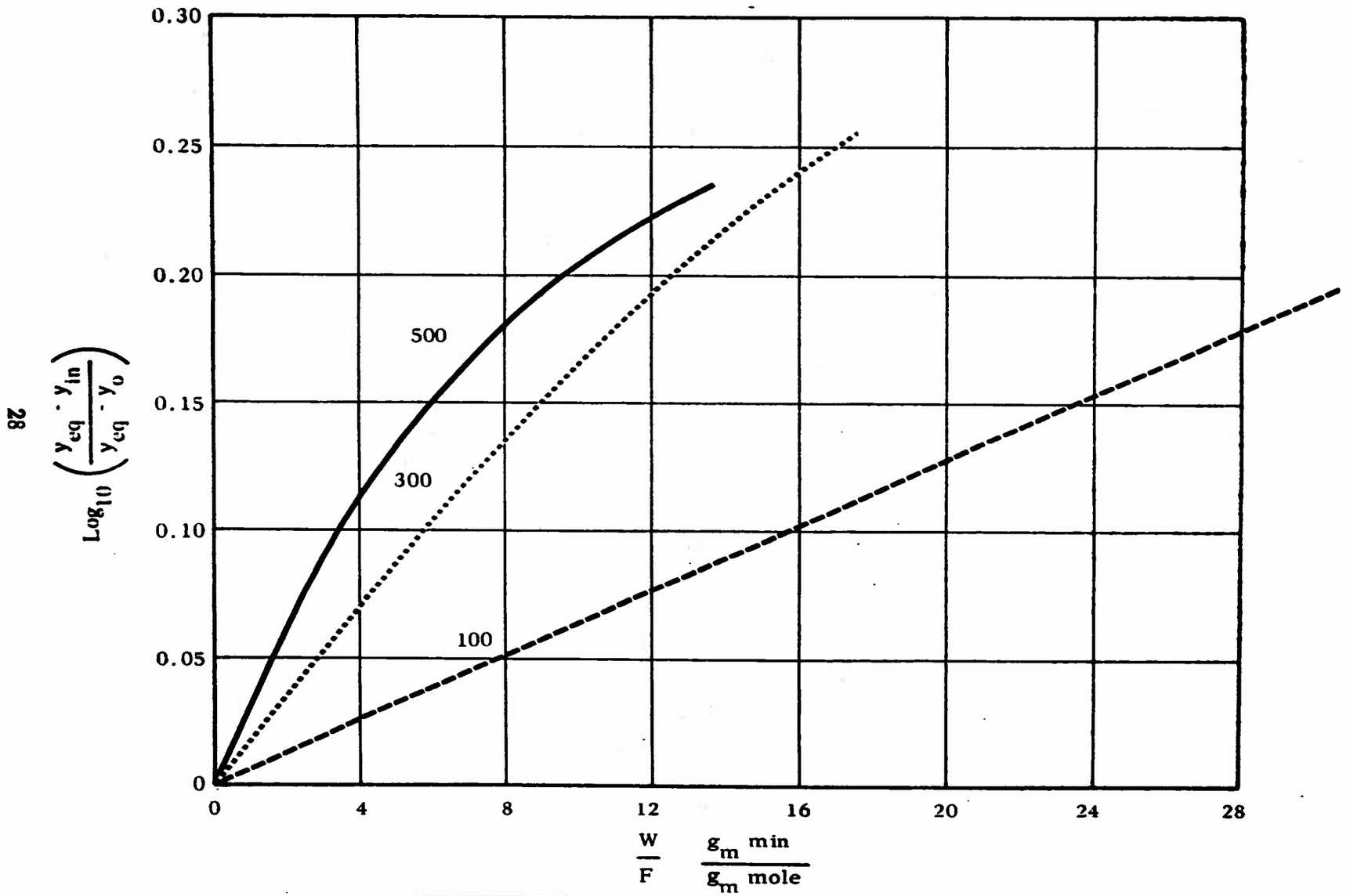

FIGURE 5 PLOT OF CATALYST ACTIVITY AS A FUNCTION OF PRESSURE FOR HYDRATED IRON OXIDE, AT -78°C SAMPLE #35

In one set of preliminary measurements made at -196°C (ortho → para conversion) it was noted that there were significant differences between the values at 500 psig and those at 300 psig, apparently because of the higher adsorption possible at lower temperatures. A typical set of data is given in Table 17 and the results are plotted in Figure 5.

TABLE 17

C. K. WILLIAMS SAMPLE NO. 35, WEIGHT 0.4696 gm, AREA 191 m^2/gm, AT -78°C

Hydrogen Pressure (psig)	Flow Rate (cc/min)	% Para	$\frac{y_{eq} - y_{in}}{y_{eq} - y_o}$	$\log_{10}\left(\frac{y_{eq} - y_{in}}{y_{eq} - y_o}\right)$	$\frac{W^*}{F}$
500	85	31.96	4.15	0.619	133.0
500	1020	40.90	1.635	0.216	11.05
500	2685	43.80	1.365	0.136	4.20
500	5285	47.26	1.143	0.058	2.14
500	8050	48.64	1.071	0.030	1.40
300	85	30.69	5.32	0.727	133.0
300	485	36.40	2.35	0.372	23.2
300	745	40.27	1.705	0.232	15.15
300	1745	44.76	1.295	0.112	6.45
300	3885	48.02	1.10	0.042	2.90
100	85	32.59	3.75	0.574	133.0
100	365	41.55	1.565	0.195	30.9
100	1365	47.36	1.136	0.056	8.25

* $\frac{\text{(gm of catalyst) (min)}}{\text{gm mole of } H_2}$

The results in terms of $K_{ov\,500}$ at -78°C for all of the catalysts run in the present work are presented in Table 18. A few preliminary runs were made at room temperature but are not included because of their small number. A number of oxides on silica gel were tested and are listed in Table 15. In addition, a set of runs of some of the more active materials was made at -196°C to test ortho → para conversion. These are not included because it was found later that the hydrogen used was sufficiently contaminated with nitrogen to deactivate the catalysts.

TABLE 18

CATALYST ACTIVITIES DURING PRESENT WORK

Sample	Activity $K_{ov\,500}$ $\frac{\text{gm mole } H_2}{(\text{gm of catalyst})(\text{min})}$ at -78°C
29	0.345
34 (AP-1)	0.346
35 (C. K. Williams)	0.0718
36	0.023
37	0.014
38	0.384
39	0.218
40	Inactive
41	0.161
42	0.0327
43	0.0575
46	0.138
47	Inactive
48	0.344
50	0.098
51	0.0502
52	0.0655
53	0.0577
54	0.487
55	0.0207
56	Inactive
57	0.622
58	Inactive
59	Inactive
60	0.391
61	0.115
63	0.173
64	0.218
65	Inactive
66	0.230
67	0.242
68	0.541
69	0.368
70	Inactive
71	0.0575
72	0.345

TABLE 18 (Continued)

Sample	Activity $K_{ov\,500}$ $\frac{\text{gm mole } H_2}{(\text{gm of catalyst})(\text{min})}$ at -78°C
73	0.205
74	Inactive
75R	0.115
76	0.276
77	0.184
78	0.760
79	0.260
80	0.161
81	0.092
82	0.207
83	0.235
84	Inactive
86	0.138
87	Inactive
89	0.047
90	0.187
91	0.135
92	Inactive
93	Inactive

2. Mercury and Helium Displacement Measurements

The pore volume measurements are given below in Table 19. The pore volumes were calculated from the relation:

$$P_v = \frac{1}{d_{He}} - \frac{1}{d_{Hg}} \qquad (16)$$

TABLE 19

VALUES OF d_{Hg}, d_{He}, P_v, AND S FOR VARIOUS CATALYSTS

Catalyst	d_{Hg} in $\frac{gm}{cm^3}$	d_{He} in $\frac{gm}{cm^3}$	P_v in $\frac{cm^3}{gm}$	S in $\frac{m^2}{gm}$
AP-1	0.995	4.290	0.772	490.
AP-1 Soaked in Boric Acid	1.055	4.075	0.703	518.6
No. 38	1.395	4.56	0.500	147.6

3. Pore Volume Distribution

We used the method of Barrett, Joyner, and Holanda,[16] which consists of an adsorption-desorption study of nitrogen on the catalyst at -195°C. (See Figure 6.) Using the original reference, we obtained the relation between P/P_0 and the multilayer thickness. We then used this relation to calculate the various quantities needed to determine the pore volume increments. For the complete details of this extended calculation, reference should be made to the original paper. In the present work, we found it necessary to calculate every angstrom unit from 20Å to 7Å in order to have the surface area match that obtained from the BET calculations. The pore volume measured in this way (0.34 ml/gm) was only half that determined by helium displacement, indicating even finer pores not accessible to nitrogen. The data for the calculations is tabulated in Table 20, and the pore volume distribution is plotted in Figure 7.

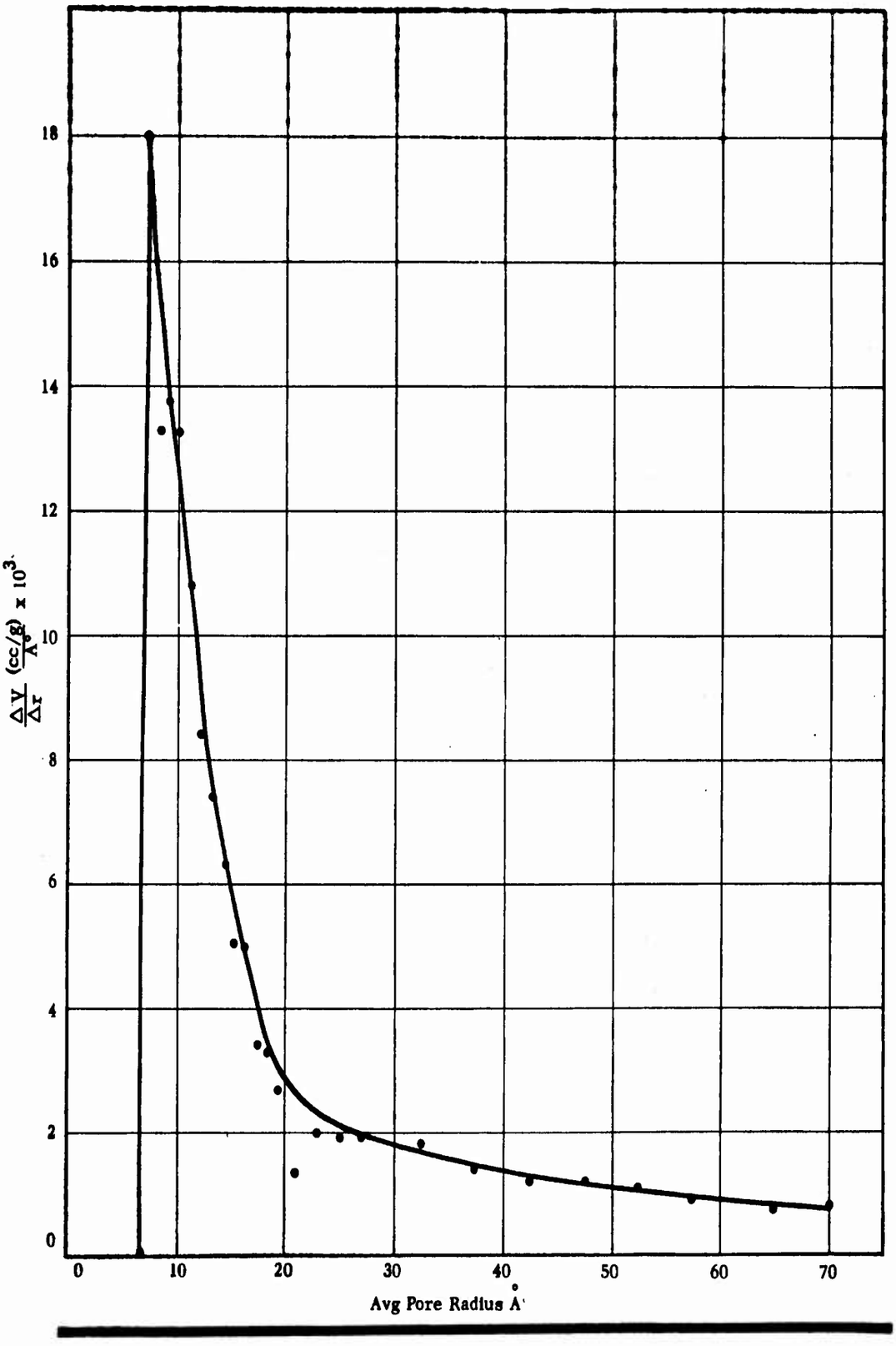

FIGURE 6 PORE VOLUME DISTRIBUTION FOR AP-1 ACTIVATED AT 285°C

TABLE 20

CALCULATED QUANTITIES OF THE PORE VOLUME DISTRIBUTION FOR AP-1

P/P_o	r_p (Å)	V_{ADS}(STP) (cm^3)	V_{ADS} Liq. (cm^3)	ΔV (cm^3)	$\bar{r}_p$ (Å)	$\Delta V \times R$	$C \times \Sigma A_p \times 10^4$	V_p (cm^3)	ΣV_p (cm^3)	A_p (m^2/gm)	ΣA_p (m^2/gm)	$\frac{\Delta V}{\Delta r}$ cc/gm/Å
0.039	7	123.7	0.1924	0.0180	7.5	0.075	0.0340	0.0412	0.3444	109.87	491.1	0.0180
0.082	8	135.3	0.2104	0.0133	8.5	0.0499	0.0246	0.0240	0.3032	57.88	381.24	0.0133
0.125	9	147.0	0.2286	0.0137	9.5	0.0472	0.0191	0.0281	0.2792	59.16	323.36	0.0137
0.165	10	155.8	0.2423	0.0133	10.5	0.0431	0.0136	0.0295	0.2511	56.19	264.20	0.0133
0.208	11	164.4	0.2556	0.0108	11.5	0.0333	0.0089	0.0244	0.2216	38.96	207.01	0.0108
0.247	12	171.3	0.2664	0.0084	12.5	0.0245	0.0070	0.0175	0.1972	28.00	168.05	0.0084
0.280	13	176.7	0.2748	0.0074	13.5	0.0207	0.0054	0.0153	0.1797	22.67	140.05	0.0074
0.313	14	181.5	0.2822	0.0063	14.5	0.0170	0.00359	0.0134	0.1644	18.50	117.38	0.0063
0.345	15	185.5	0.2885	0.0051	15.5	0.0131	0.00281	0.0103	0.1510	13.28	98.88	0.0051
0.375	16	188.8	0.2936	0.0050	16.5	0.0124	0.00231	0.0101	0.1408	12.12	85.60	0.0050
0.406	17	192.0	0.2986	0.0034	17.5	0.0081	0.00216	0.0059	0.1299	6.74	73.48	0.0034
0.433	18	194.2	0.3020	0.0032	18.5	0.0074	0.00190	0.0055	0.1240	5.95	66.74	0.0032
0.462	19	196.3	0.3052	0.0027	19.5	0.0061	0.00210	0.0040	0.1185	4.10	60.79	0.0027
0.488	20	198.0	0.3079	0.0031	21	0.0067	0.00255	0.0042	0.1145	3.95	56.69	0.00135
0.520	22	200.0	0.3100	0.0039	23	0.0080	0.00259	0.0054	0.1094	4.70	52.64	0.00195
0.560	24	202.5	0.3149	0.0039	25	0.0078	0.00228	0.0055	0.1040	4.42	47.94	0.00195
0.593	26	205.0	0.3188	0.0039	27	0.0076	0.0020	0.00568	0.0985	4.13	43.52	0.00195
0.620	28	207.3	0.3255	0.0039	29	0.0070	0.0014	0.00557	0.0929	3.84	39.39	0.00195
0.642	30	209.0	0.3250	0.0093	32.5	0.0166	0.0029	0.0137	0.0873	8.43	35.55	0.0018
0.693	35	215.3	0.3343	0.0070	37.5	0.0120	0.0019	0.0101	0.0736	5.39	27.12	0.0014
0.725	40	219.5	0.3413	0.0062	42.5	0.0102	0.0014	0.0088	0.0635	4.14	21.73	0.0012
0.775	50	227.5	0.3538	0.0054	52.5	0.0084	0.0007	0.0077	0.0456	2.93	13.76	0.0011
0.795	55	231.0	0.3592	0.0046	57.5	0.0070	0.0005	0.0065	0.0379	2.26	10.83	0.0009
0.810	60	234.0	0.3638	0.0078	65	0.0115		0.0115	0.0314	3.54	8.57	0.0078
0.860	90	243.0	0.3779	0.0063	85	0.0088		0.0088		2.07	2.07	0.0063
0.875	90										0	

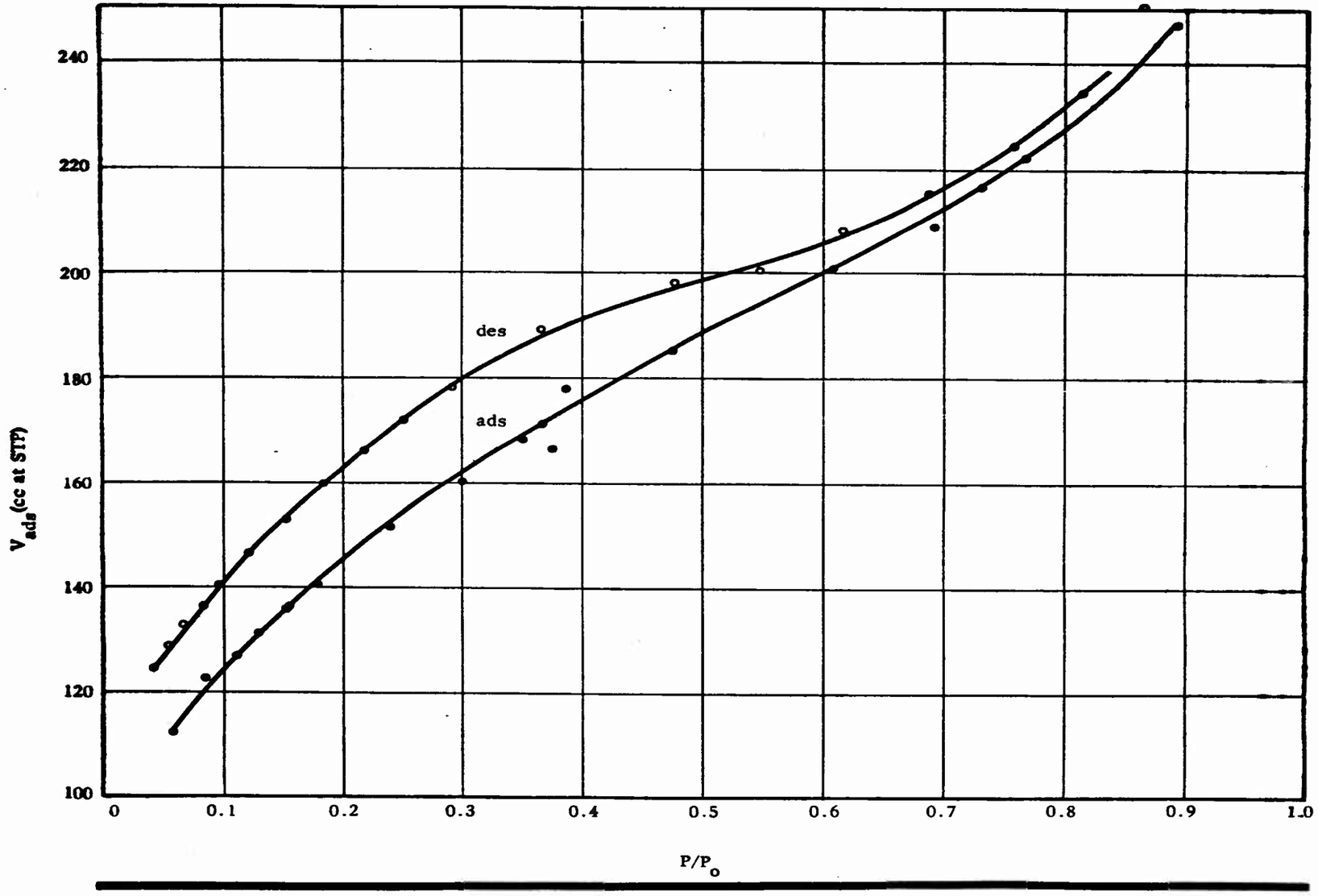

FIGURE 7 PLOT OF ADSORPTION AND DESORPTION OF NITROGEN ON AP-1

IV. CONCLUSIONS AND RECOMMENDATIONS

A. CONCLUSIONS

1. A series of catalysts that are up to ten times more active than a standard iron oxide catalyst for para-ortho hydrogen catalysis have been developed.

2. The activity of para-ortho hydrogen catalysts is significantly affected by radiation but prediction of the effect is not possible based on existing theory.

3. At the temperatures and pressures of use of this para-ortho hydrogen conversion, the effective diffusivities of the catalysts are determined by both Knudsen and bulk diffusion.

B. RECOMMENDATIONS

1. A systematic investigation into the effects of the variables encountered in the preparation of a selected number of the active catalysts be undertaken in order to optimize their activity.

2. Basic theoretical studies be started to provide a better understanding of the theory of para-ortho hydrogen catalysts.

APPENDIX

CALCULATION OF RATE OF EQUILIBRATION OF PARA-ORTHO HYDROGEN IN CYLINDER

The cylinder is a stainless-steel vessel with a radius of 6.81 cm and contains a cylinder of catalyst with a radius of 0.5 cm. After evacuation to a specified pressure, hydrogen is put into the cylinder and the cylinder is cooled to -196°C. The cylinder is then allowed to stand until equilibration takes place. This is treated as a diffusion-controlled reaction with the assumption that the hydrogen is equilibrated as soon as it comes in contact with the catalyst. The diffusion equation is:

$$\frac{D}{r}\frac{\partial}{\partial r}\left(r\frac{\partial n}{\partial r}\right) = \frac{\partial n}{\partial t} \qquad a < r < b \tag{17}$$

where

r = radius

D = coefficient of diffusion

n = concentration of para H_2

This is Bessel's equation, and since $r > o$, Bessel functions of the second type cannot be excluded. Therefore, the solution has the form:

$$n(r, t) = B + C_1 e^{-\frac{\beta^2 Dt}{b^2}}\left[A_1 J_o\left(\frac{\beta r}{b}\right) + A_2 Y_o\left(\frac{\beta r}{b}\right)\right] \tag{18}$$

where

$B = n_o$ = starting concentration of parahydrogen and we have retained only the first two terms of the general solution.

The boundary conditions are:

$$1.\ n(a, t) = n_c \tag{19}$$

where a = radius of catalyst cylinder

n_c = equilibrium concentration of parahydrogen

$$2.\ \frac{\partial n}{\partial r}\ (b,\ t) = o \tag{20}$$

where b = outer radius

This indicates that the concentration gradient at the outer wall is 0 because there is no flow.

$$3.\ n(r,\ 0) = n_o \tag{21}$$

$$\text{At any time } t:\quad A_1 J_o\left(\frac{\beta a}{b}\right) + A_2 Y_o\left(\frac{\beta a}{b}\right) = 0 \tag{22}$$

$$\text{For } \frac{\partial n}{\partial r}\ (b,\ t) = 0:\quad A_1 J_o'(\beta) + A_2 Y_o'(\beta) = 0 \tag{23}$$

$$\text{Therefore,}\quad \frac{J_o'(\beta)}{Y_o'(\beta)} = \frac{J_o\left(\frac{\beta a}{b}\right)}{Y_o\left(\frac{\beta a}{b}\right)} = \frac{J_1(\beta)}{Y_1(\beta)} \tag{24}$$

Substituting the values for a and b and plotting the values of

$$\frac{J_o\left(\frac{\beta a}{b}\right)}{Y_o\left(\frac{\beta a}{b}\right)} \text{ and } \frac{J_1(\beta)}{Y_1(\beta)} \text{ calculated from}$$

Jahnke and Emde[17] and shown in Figure 8, the solution $\beta = 1.07$ is determined. The time required for the concentration at b to reach $\frac{1}{e}$ of that at the center is:

$$\tau = \frac{b^2}{\beta^2 D} \tag{25}$$

This can be solved based on values of D. D can be calculated from formulas derived in Hirschfelder.[18]

$$D = \frac{0.002628\left[\frac{T^3}{M}\right]^{1/2}}{P\sigma^2\Omega^{(1,1)^*}(T^*)} \tag{26}$$

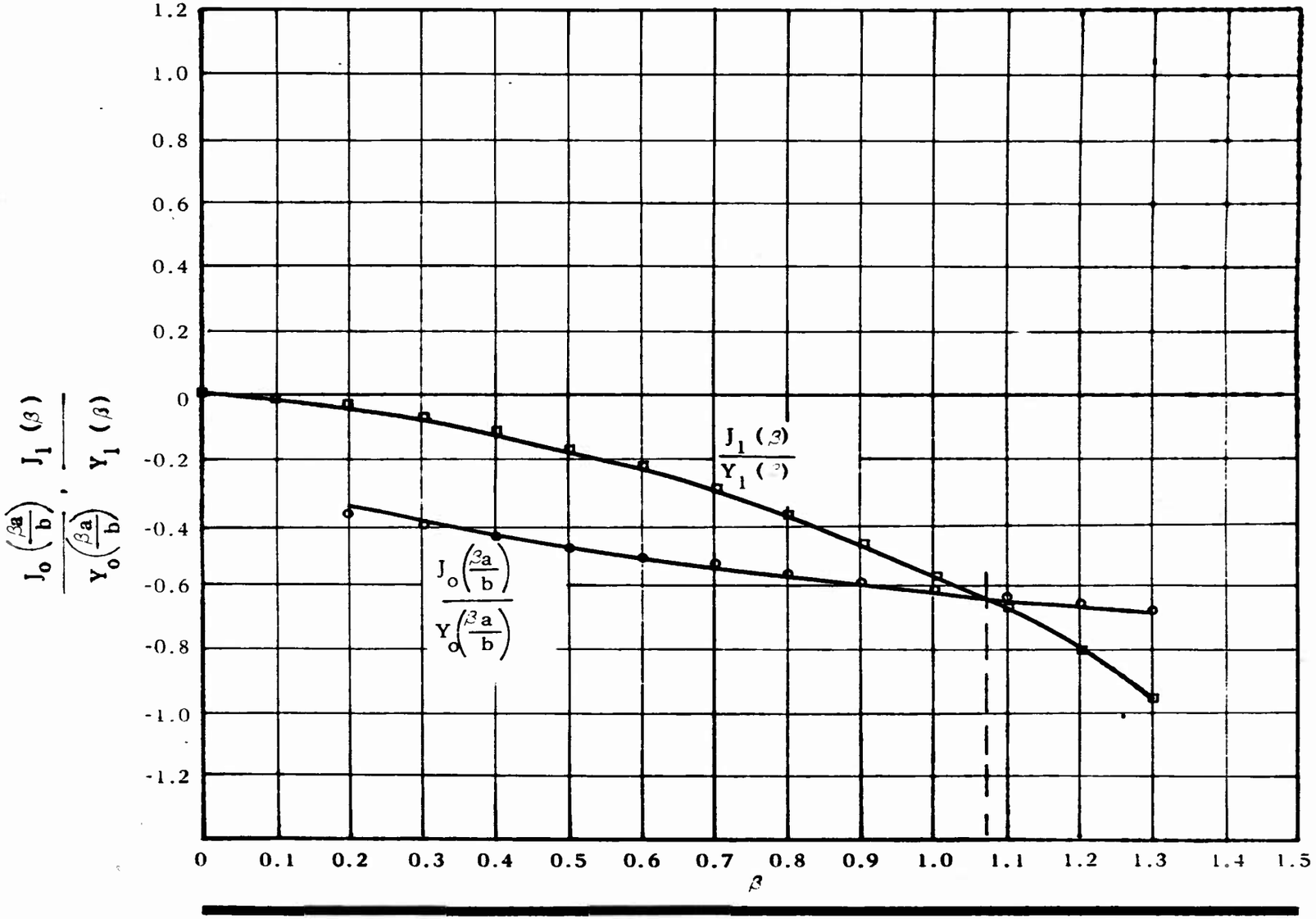

FIGURE 8 PLOT OF $\frac{J_o\left(\frac{\beta a}{b}\right)}{Y_o\left(\frac{\beta a}{b}\right)}$ AND $\frac{J_1(\beta)}{Y_1(\beta)}$

where $T^* = \frac{kT}{\varepsilon}$

M = molecular weight

$\Omega^{(1,1)^*}$ = value obtained from tables

σ = collision radius

P = pressure in atmospheres

For H_2: $M = 2$

$T = 77$

$T^* = \frac{77}{29.2} = 2.64$

$\Omega^{(1,1)^*} = 0.9836$

$\sigma = 2.87$

For P = 50 atmospheres:

$$D = \frac{0.002628 \left[\frac{77^3}{2}\right]^{1/2}}{(2.87^2)(0.9836)(50)}$$

$$= 0.00312 \frac{cm^2}{sec}$$

Using this to find τ:

$$\tau = \frac{\left(\frac{5.37 \times 2.54}{2}\right)^2}{1.07^2 \times 0.00312}$$

$$= 13,130 \text{ seconds or } 3.65 \text{ hours}$$

For $e^{-\frac{t}{\tau}} = 0.01 = 1\%$ from equilibrium where we set $C_1 = 1$,

$$t = 4.6 \times 3.65 = 16.8 \text{ hours}$$

This is a maximum value based on diffusion alone and probably is high since there will be some convection. To be safe, the cylinder is allowed to stand several days at 77°K before any hydrogen is used.

Calculation of Error Caused by Setting $C_1 = 1$.

The actual form of the solution to Bessel's equation is:

$$n(r, t) = n_c + \Sigma_i C_i e^{-\frac{\beta_i^2 Dt}{b^2}} \left[J_o\left(\frac{\beta_i r}{b}\right) + \gamma Y_o\left(\frac{\beta_i r}{b}\right) \right] (n_o - n_c) \qquad (27)$$

At $t = o$, $n = n_o$

$$\therefore \Sigma_i C_i \left[J_o \frac{\beta_i r}{b} + \gamma Y_o \left(\frac{\beta_i r}{b}\right) \right] = 1 \qquad (28)$$

$$\text{where } \gamma = -\frac{J_1(\beta_i)}{Y_1(\beta_i)}$$

Now,

$$\int_a^b \left[J_o\left(\frac{\beta_k r}{b}\right) + \gamma Y_o\left(\frac{\beta_k r}{b}\right) \right] r\,dr = \Sigma_i C_i \int_a^b \left[J_o\left(\frac{\beta_i r}{b}\right) + \gamma Y_o\left(\frac{\beta_i r}{b}\right) \right] \cdot \left[J_o\left(\frac{\beta_k r}{b}\right) + \gamma Y_o\left(\frac{\beta_k r}{b}\right) \right] r\,dr \qquad (29)$$

Because of orthogonality relations, the right hand expression equals:

$$\sum_i C_k \int_a^b \left[J_o\left(\frac{\beta_k r}{b}\right) + \gamma Y_o\left(\frac{\beta_k r}{b}\right) \right]^2 r\,dr$$

$$\text{And } C_k = \frac{\int_a^b \left[J_o\left(\frac{\beta_k r}{b}\right) + \gamma Y_o\left(\frac{\beta_k r}{b}\right) \right] r\,dr}{\sum_i \int_a^b \left[J_o\left(\frac{\beta_k r}{b}\right) + \gamma Y_o\left(\frac{\beta_k r}{b}\right) \right]^2 r\,dr}$$

If t is large, all $k > 1$ can be neglected.

$$\therefore n(r, t) = n_c + C_1 \left[J_o\left(\frac{\beta_1 r}{b}\right) + \gamma Y_o\left(\frac{\beta_1 r}{b}\right) \right] e^{-\frac{\beta_1^2 Dt}{b^2}} (n_o - n_c) \qquad (30)$$

$$\text{and } \bar{n}(t) = \frac{2}{b^2 - a^2} \int_a^b n(r, t)\, r\, dr$$

$$= \frac{2}{b^2 - a^2} (n_o - n_c) e^{-\frac{\beta_1^2 Dt}{b^2}} \int_a^b \left[J_o\left(\frac{\beta_1 r}{b}\right) + \gamma Y_o\left(\frac{\beta_1 r}{b}\right) r\, dr \right] + n_c$$

$$= \frac{2}{b^2 - a^2} (n_o - n_c) e^{-\frac{\beta_1^2 Dt}{b^2}} \frac{\left[\int_a^b J_o\left(\frac{\beta_1 r}{b}\right) + \gamma Y_o\left(\frac{\beta_1 r}{b}\right) r\, dr \right]^2}{\int_a^b \left[J_o\left(\frac{\beta_1 r}{b}\right) + \gamma Y_o\left(\frac{\beta_1 r}{b}\right) \right]^2 r\, dr} \qquad (31)$$

This was evaluated by graphical integration, as shown in Figures 9 and 10.

$$\bar{n}(t) = (n_o - n_c) e^{-\frac{\beta_1 Dt}{b^2} \left(\frac{16.44^2}{23.05 \times 12.57} \right)}$$

$$= 0.937 (n_o - n_c) e^{-\frac{\beta_1 Dt}{b^2}} \qquad (32)$$

Therefore, the corrected equation is almost the same as that assumed with $C_1 = 1$, and the error is negligible.

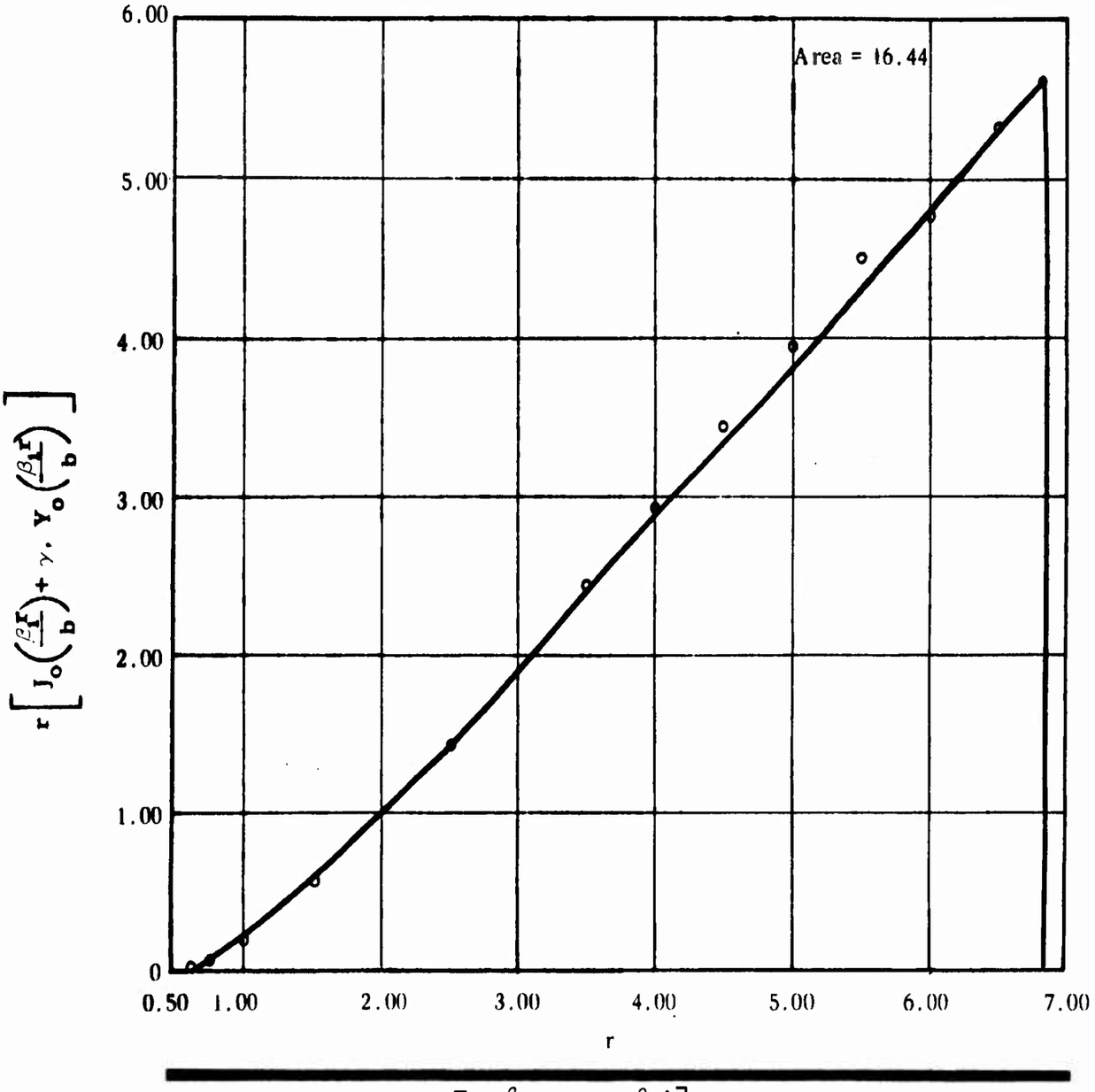

FIGURE 9 PLOT OF $\left[J_o\left(\frac{\beta_1 r}{b}\right)+\gamma Y_o\left(\frac{\beta_1 r}{b}\right)\right]r$ VS r

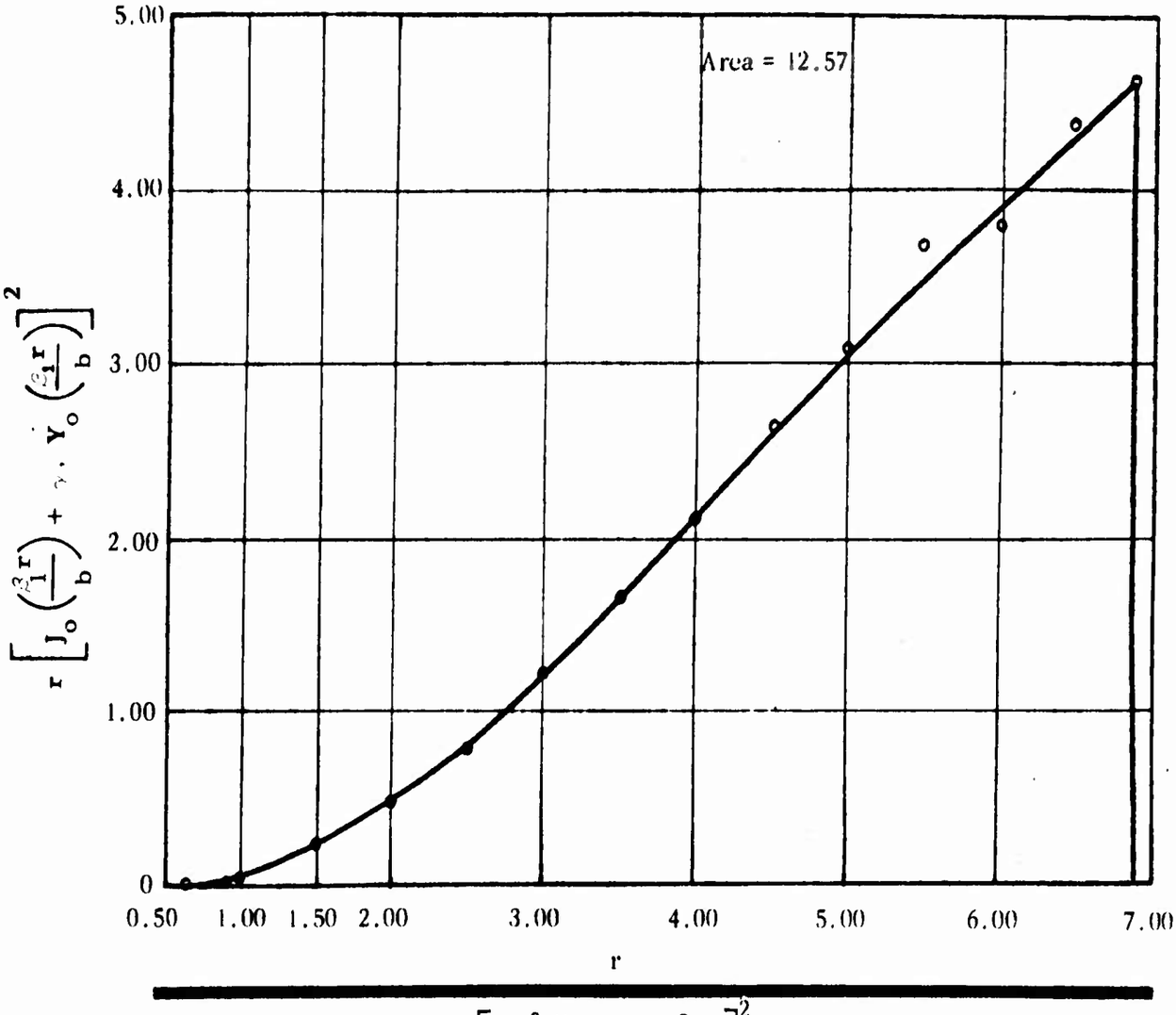

FIGURE 10 PLOT OF $\left[J_o\left(\frac{\beta_1 r}{b}\right) + \cdot Y_o\left(\frac{\beta_1 r}{b}\right)\right]^2 r$ VS r

REFERENCES

1. Wigner, E., Z. Physik. Chem., B23, 28 (1933).

2. Kalckar, F. and Teller, E., Proc. Roy. Soc., A150, 520 (1935).

3. Selwood, P. W., Adsorption and Collective Paramagnetism, Academic Press, New York, 1962.

4. Coekelbergs, R., Crucq, A., and Frennet, A., Advances in Catalysis, Vol. 13. Academic Press, New York, 1962, Chapter 2.

5. Cropper, W.H., Science, 137, 955 (1962).

6. Hoigne, J. and Ballantine, D. J., App. Radiation and Isotopes, 14, 221 (1963).

7. Sturge, M. D. Phys. Rev., 130, 639 (1963).

8. Voska, K., and Di Luzio, J. W., J. Amer. Chem. Soc., 84, 679 (1962).

9. Satterfield, C. N., and Sherwood, T. K., The Role of Diffusion in Catalysis, to be published; Wheeler, A., Advances in Catalysis, Vol. 3, Academic Press, New York, 1951, pp. 249-327.

10. Noller, H., Andreu, P., and Schwab, G. M., Z. Physik. Chem., Neue Folge, 36, 179 (1963).

11. Weisz, P. B., and Schwartz, A. B., J. of Catalysis, 1, 399 (1962).

12. McKinley, C., and Schmauch, G., Paper presented at Cryogenic Engineering Conference, Boulder, Colorado, August 1963. We wish to thank Dr. Schmauch for making the preprint available.

13. For a discussion, see Catalysis, Vol. 1, Reinhold, New York, 1954, Chapters 3, 4.

14. Wakao, N., Smith, J. M., and Selwood, P. W., J. of Catalysis, 1, 62-73 (1962); Wakao, Selwood, P. W., and Smith, J. M., Am. Inst. Chem. Engrs. J., 8, 478-81 (1962).

15. Rossman, R. P., and Smith, W. R., Ind. Eng. Chem., 35, 972 (1943).

REFERENCES (Continued)

16. Barrett, E. P., Joyner, L. G., and Holanda, P. P., J. Amer. Chem. Soc., 73, 373 (1951).

17. Jahnke and Emde, Tables of Functions, Dover, New York, 1943.

18. Hirshfelder, J. O., Curtiss, C. F., and Bird, R. B., Molecular Theory of Gases and Liquids, John Wiley, New York, 1954.

DISTRIBUTION LIST

Wright-Patterson AFB
ASRPR (4 copies)
ASRMPE (Mr. R. E. Supp)
ASNRTP (Dave McHenry)
ASRPF-10 (50 copies)
ASRSMX-10

AFBMD (WDZC)
Det. #2
AF Unit Post Office
Los Angeles 45, California

Armed Services Technical Information Agency
Arlington Hall Station
Arlington 12, Virginia (30 copies)

Arnold Engineering Development Center
ATTN: AEGP
Tullahoma, Tennessee

NASA
Lewis Research Center
ATTN: Mr. A. Silverstein
21000 Brookpark Road
Cleveland 35, Ohio

NASA
George C. Marshall Space Flight Center
ATTN: Dr. W. R. Lucas
Huntsville, Alabama

National Bureau of Standards
Cryogenic Engineering Laboratory
ATTN: R. B. Scott
Boulder, Colorado (3 copies)

National Bureau of Standards
ATTN: Thermodynamics Section
Washington 25, D.C.

Naval Air Materials Center
Naval Experimental Station
ATTN: Director
Philadelphia 12, Pa.

Pratt & Whitney Aircraft
Division of United Aircraft Corporation
ATTN: G. J. Andreini
East Hartford 8, Connecticut

Aerojet General Corporation
Department 953, Building 160
ATTN: Library
Box 296
Azusa, California

Naval Ordnance Laboratory
White Oak, Maryland

Aerojet General Corporation
ATTN: Technical Information Office
P.O.Box 1947
Sacramento, California

Air Products, Incorporated
P.O.Box 538
ATTN: Mr. George E. Schmauch
Allentown, Pa.

AiResearch
Division of Garrett Corporation
ATTN: R. Dunzwzy, C. Paul,
M. McKenzie
402 South 38th Street
Phoenix, Arizona

AiResearch
Division of Garret Corporation
ATTN: L. Fullerton, H. Titzler,
W. Melber, G. Mlauaka, R. Fischer,
H. Walters
Los Angeles 45, California (2 copies)

Atlantic Research Corporation
ATTN: Mike Markel
Shirley Highway and Edsall Road
Alexandria, Va.

The Dynatech Corporation
ATTN: Mr. J. P. Barger
17 Tudor Street
Cambridge, Mass.

The Marquardt Corporation
ATTN: Mr. Howard McFarland
16555 Sticoy Street
Van Nuys, California

General Motors Research Laboratories
ATTN: Mr. P. T. Vichera
P.O.Box 272
Warren, Michigan

The Boeing Company
Aerospace Division
ATTN: Mr. J. D. Alexander, Mail Stop 04072
Box 3707
Seattle, Washington

Douglas Aircraft Company, Inc.
Santa Monica Division
ATTN: Mr. Anthony A. DuPont
3000 Ocean Park Blvd.
Santa Monica, California

Lockheed Aircraft Division
California Division
ATTN: Mr. J. G. Krisiles
Burbank, California

North American Aviation, Inc.
Space and Information Systems Division
ATTN: Dr. W. R. Laidlaw
12214 Lakewood Blvd.
Downey, California

General Electric Company
ATTN: Mr. D. F. Jamison
Flight Propulsion
118 W. First Street
Dayton 2, Ohio

Republic Aviation Corporation
ATTN: Mr. Vincent Tizsio
Applied Research and Development Div.
Farmingdale, Long Island, New York

Pratt & Whitney Aircraft
Division of United Aircraft Corporation
Florida Research and Development Center
ATTN: Mr. Peter Klitjaard
West Palm Beach, Florida

The Linde Company
Tonawanda Laboratories
ATTN: Mr. Mark O. Johnson
61 East Park Drive
Tonawanda, New York

General Dynamics
P.O.Box 2676
ATTN: Mr. S. Campbell
San Diego 12, California

The Boeing Company
ATTN: Bob Page, Mail Stop 1443
Aerospace Division
Seattle, Washington

Texaco Experimental, Inc.
Richmond 2, Virginia

Dow Chemical Company
644 Midland Building
Midland, Michigan

Curtiss-Wright Corporation
Wright Aeronautical Division
ATTN: Mr. S. Lombardo
Engineering Department
Wood-Ridge, New Jersey

Arthur D. Little, Inc.
ATTN: A. J. Leffler
Acorn Park
Cambridge 40, Mass.

Arthur D. Little, Inc.
ATTN: R. B. Hinckley
Acorn Park
Cambridge 40, Mass.

Garrett Corporation
AiResearch Manufacturing Company
Heat Transfer Department (93-5)
ATTN: Mr. Frank Carroll
9851 Sepulveda Blvd.
Los Angeles, California

Headquarters, USAF
Room 4B341
ATTN: AFDRT-AS (Mr. Al Eaffy)
The Pentagon
Washington 25, D.C.

AFCRC (CROT)
ATTN: Technical Library
Hanscom Field, Mass.

AFFTC (FTRPL)
Edwards Air Force Base
California (2 copies)

AFSC (SCMK-5)
Andrews AFB
Washington 25, D.C.

Bureau of Mines
Department of the Interior
ATTN: Mr. R. W. VanDolak
4800 Forbes Avenue
Pittsburgh 13, Pa.

Bureau of Mines
Department of the Interior
ATTN: T. R. Scollon
Washington 25, D.C.

Federal Aviation Agency
ATTN: Library
Washington 25, D.C.

Library of Congress
Air Information Service
Washington 25, D.C.

NASA
Langley Research Center
Langley Field, Virginia

National Bureau of Standards
Dept. of Commerce
ATTN: Dr. A. F. Robertson
Washington 25, D.C.

U.S. Army Air Defense Unit
Fort Bliss
Texas

U.S. Atomic Energy Commission
P.O. Box 5400
Albuquerque, New Mexico

U.S. Atomic Energy Commission
Technical Information Service
P.O. Box 62
Oak Ridge, Tennessee

U.S. Atomic Energy Commission
Technical Information Service
1901 Constitution Avenue
Washington 25, D.C.

ACF Industries, Incorporated
Box 5
Riverside, Maryland

Aerojet General Corporation
ATTN: Technical Information Office
P.O. Box 1947
Sacramento, California

Allen B. Dumont Laboratories, Inc.
11800 Olympic Boulevard
Los Angeles 64, California

Allied Research Associates
43 Leon Street
Boston 15, Mass.

Allison Division
General Motors Corp.
ATTN: Library
Box 894
Indianapolis 6, Indiana

American Machine & Foundry Co.
1025 N. Royal Street
Alexandria, Virginia

Argonne National Laboratory
9700 South Cass Avenue
Argonne, Illinois

Armour Research Foundation
10 West 35th Street
Chicago 16, Illinois

AVCO Manufacturing Corporation
1329 Arlington Street
Cincinnati 25, Ohio

AVCO Research Library
2385 Revere Beach Parkway
Everett 49, Mass.

Battelle Memorial Institute
505 King Avenue
Columbus, Ohio

Bendix Corporation
Pioneer-Central Division
ATTN: Dr. Thomas M. Flynn
Davenport, Iowa

Bendix Aviation Corporation
401 Bendix Drive
South Bend 20, Indiana

Boeing Airplane Company
ATTN: Mr. Henry Walker
224 North Wilkinson
Dayton, Ohio

Boeing Airplane Company
ATTN: Mr. Charles Duffer
Wichita Division
Wichita, Kansas

Borg Warner Corp.
Research Center
Des Plaines, Illinois

Brookhaven National Laboratory
ATTN: Mr. L. A. Baker
Upton, Long Island
New York

California Institute of Technology
1201 California Street
Pasadena 4, California

Callery Chemical Company
Callery, Pennsylvania

Carnegie Institute of Technology
Metals Research Laboratory
ATTN: Dr. C. L. McCabe
Schenley Park
Pittsburgh 13, Pennsylvania

Chemical Thermodynamic Properties Center
Department of Chemistry
A & M College of Texas
ATTN: Dr. B. J. Zwolinski
College Station, Texas

Consolidated Electrodynamics Corp.
300 North Sierra Madre Villa
Pasadena, California

Convair
Division of General Dynamics Corp.
Forth Worth, Texas

Convair Division
General Dynamics Corp.
ATTN: Mr. Dick Nav
San Diego, California

Convair - Astronautics
P.O.Box 1128
ATTN: Mr. G. D. Davis
5001 Kearny Villa Road
San Diego 12, California

Cornell Aeronautical Laboratory
4455 Genesee Street
P.O.Box 235
Buffalo 21, New York

Cornell University
Department of Chemistry
Ithaca, New York

Courtney and Company
1711 Walnut Street
Philadelphia 3, Pennsylvania

Wright Aeronautical Division
Curtis-Wright Corporation
ATTN: Technical Library
Woodridge, New Jersey

Douglas Aircraft Company, Inc.
Long Beach Division
ATTN: Mr. R. E. Bates
Long Beach, California

Douglas Aircraft Company, Inc.
3000 Ocean Park Boulevard
Santa Monica, California

Chrysler Corporation
ATTN: Library, Missile Division
Box 2628
Detroit 31, Michigan

Clifford Manufacturing Co.
Division of Standard Thompson Corp.
578 Grove Avenue
Waltham, Massachusetts

Colgate University
Department of Chemistry
ATTN: Eugene Clark, Dr. A. S. Brown
Hamilton, New York

Fairchild Engine and Airplane
Corporation
Stratos Division
Orinoco Drive
Bay Shore, Long Island, New York

Electro-Optical Systems, Inc.
3016 East Foothill Boulevard
Pasadena, California

Fairchild Aircraft Company
Division of Fairchild Engine and
and Airplane Corporation
ATTN: Mr. W. Taylor
Hagerstown, Maryland

General Electric Company
P.O.Box 196
Cincinnati, Ohio

Franklin Institute
Research and Development Laboratory
20th and Parkway Streets
Philadelphia 3, Pennsylvania

Ford Motor Company
Research and Engineering Center
ATTN: Technical Information Section
2000 Rotunda Drive
Dearborn, Michigan

General Motors Technical Center
ATTN: Charles A. Chayne
Box 177 - North End Station
Detroit, Michigan

Dow Chemical Company
644 Midland Building
Midland, Michigan

DuPont Corporation
3500 Greys Ferry Avenue
Philadelphia 46, Pennsylvania

DuPont Corporation
Jackson Laboratory
Box 525
Wilmington 99, Delaware

Ethyl Corporation
1600 West Eight Mile Road
Ferndale 20, Michigan

General Precision Laboratory
ATTN: Mr. Cambell
63 Bedford Road
Pleasantville, New York

George Washington University
707 22nd Street, N.W.
Washington 7, D.C.

Giannini Controls Corporation
ATTN: Mr. Jack Hoog (B.C. Beach)
1600 South Montain Avenue
Duarte, California

Giannini Controls Corporation
ATTN: Mr. A. Moncrieff - Yeates
2275 East Foothill Boulevard
Pasadena, California

Goodyear Aircraft Corporation
Litchfield Park, Arizona

Grisom - Russel
Massilon, Ohio

Grumman Aircraft Engineering Corp.
Bethpage, Long Island, New York

General Dynamics Corporation
Electric Boat Division
ATTN: Mr. A. Bialecki
Groton, Connecticut

General Motors Corporation
Defense Systems Division
ATTN: Dr. R. B. Costello
P.O.Drawer T
Santa Barbara, California

Kentucky Research Foundation
Wenner-Gren Aeronautical Laboratory
University of Kentucky
Lexington, Kentucky

Walter Kidde and Co., Inc.
Kidde Aero-Space Division
ATTN: Mr. K. Traynelis
Belleville 9, New Jersey

Lear, Inc.
110 Ionia Avenue
Grand Rapids 2, Michigan

Linde Company
Speedway Laboratory
ATTN: Mr. John Bechman
Speedway, Indiana

Linde Company Division
Union Carbide Corporation
ATTN: Warren E. Perkins
61 East Park Drive
Tonawanda, New York

Lockheed Aircraft Corporation
3333 Middlefield Road
Menlo Park, California

Lockheed Aircraft Corporation
ATTN: Mr. Harry Drell
Department 72-75
Box 551
Burbank, California

Hayes Aircraft Company
Box 2287
Birmingham, Alabama

Hercules Powder Company
Box 210
Cumberland, Maryland

Hughes Aircraft Company
Florence and Teale Streets
ATTN: Dr. Warren Mathews
Culver City, California

Hughes Aircraft Company
Research Division
ATTN: H. Ims
Malibu Beach, California

Hughes Aircraft Company
P. O. Box 11337
Emery Park Station
Tucson, Arizona

Johns Hopkins University
Applied Physics Laboratory
ATTN: Harold S. Rienstra
8621 Georgia Avenue
Silver Spring, Maryland - 2 cys

Linde Company Division
Union Carbide Corporation
ATTN: Dr. E. L. McCawdless
270 Park Ave., New York, New York

Glenn L. Martin Company
ATTN: Mr. Bitner
Baltimore 3, Maryland

Martin Company
Box 179
Denver, Colorado

Massachusetts Institute of Technology
Naval Supersonic Laboratory
560 Memorial Drive
Cambridge, Massachusetts - 3 cys

Los Alamos Scientific Laboratory
"N" Division
ATTN: Dr. Schreiber
P.O.Box 1663
Los Alamos, New Mexico

Lockheed Aircraft Corporation
Marietta, Georgia

Logan Lewis Library
Carrier Parkway
Syracuse 1, New York

The Marquardt Corporation
Library
ATTN: Mary Burdett
16555 Saticoy Street
Van Nuys, California

The Marquardt Corporation
ATTN: Mr. H. McFarland
16555 Saticoy Street
Van Nuys, California

Northwestern University
Department of Chemical Research
Evanston, Illinois

Ohio State University
Cryogenics Laboratory
Columbus 10, Ohio

Ohio State University
Library
Columbus 10, Ohio

Olin Mathieson Chemical Corporation
ATTN: Dr. Donald R. Martin
High Energy Fuel Division
P.O.Box 438
Niagara Falls, New York

Ontario Research Foundation
Department of Chemistry
43 Queen's Park
Toronto 5, Ontario, Canada

McDonnell Aircraft Corporation
Box 516
ATTN: Engineering Library
St. Louis 66, Missouri

McGraw-Hill Book Company
330 West 42nd Street
New York 36, New York

Melpar, Inc.
43 Leon Street
Boston 15, Massachusetts

Melpar, Inc.
3000 Arlington Boulevard
Falls Church, Virginia

Metal Hydrides, Inc.
ATTN: Dr. Johnson
Beverly, Massachusetts

Minneapolis Honeywell Aeronautical Div.
ATTN: Library
2600 Ridgeway Road
Minneapolis 13, Minnesota

National Carbon Research Laboratory
Box 6116
Cleveland 1, Ohio

National Science Foundation
Office of Scientific Information
Washington 25, D.C.

New York University
Department of Chemical Engineering
New York 53, New York

North American Aviation, Inc.
ATTN: Mr. Ken Keate
118 West First Street
Dayton 2, Ohio

Northern Research and Engineering Corp.
ATTN: Kymus Ginwala
283 Main Street
Cambridge, Massachusetts

Pennsylvania State University
Department of Chemistry
ATTN: Dr. Thomas Wartik
University Park, Pennsylvania

Peaco Products Division
Borg-Warner Division
ATTN: Miss Clark, Engineering Dept.
Bedford, Ohio

Phillips Petroleum Company
ATTN: Library
Chemical Laboratory Building
Bartlesville, Oklahoma

Polytechnical Institute of Brooklyn
Brooklyn, New York

Pratt & Whitney
United Aircraft Corporation
ATTN: Mr. Walter Doe
Main Street
East Hartford, Connecticut

Pratt & Whitney Division
United Aircraft Corporation
Florida Research and Development Center
ATTN: Mr. R. C. Mulready
United, Florida

Pratt & Whitney Aircraft Division
Florida Research and Development Center
ATTN: Mr. Richard Coar
Box 2691
West Palm Beach, Florida

Shell Oil Company
Box 262
Wood River, Illinois

Solar Aircraft Company
2200 Pacific Highway
San Diego 12, California

Southwest Research Institute
ATTN: Mr. P. M. Ku
Box 2296
San Antonio, Texas

Prengle Dulker and Crump
Houston, Texas

Princeton University
Department of Aeronautical Engineering
Princeton, New Jersey

Purdue University
Lafayette, Indiana

R.C.A. Victor, Ltd.
1001 Lenoir Street
Montreal 30, Canada

Redel, Incorporated
ATTN: Mr. D. C. Vest
220 North Atchinson Street
Anaheim, California

Research, Inc.
115 North Buckerman Avenue
Hopkins, Minnesota

Rocket Power/Talco
ATTN: Mr. John Elden
P.O.Box 231
Mesa, Arizona

Rocket Power/Talco Research
Laboratory
ATTN: Milton Farber
3016 East Foothill Boulevard
Pasadena, California

Rocket Research
233 Holden Street
Seattle, Washington

Rohm and Haas
Redstone Arsenal Research Division
Huntsville, Alabama

Ryan Aeronautical Corporation
Lindberg Field
San Diego, California

Sandia Corporation
Box 5800
Albuquerque, New Mexico

Stanford Research Institute
711 14th Street, N.W.
Washington 25, D.C.

Stauffer Chemical Company
ATTN: Dr. J. T. Bashovr
Chauncey, New York

Stauffer Chemical Company
1375 South 47th Street
Richmond 4, California

Stewart-Warner Corporation
South Wind Division
1514 Drover Street
Indianapolis, Indiana

Sunstrand Corporation
2480 West 70th Avenue
Denver 21, Colorado

Aviation Division
Sunstrand Corporation
ATTN: Mr. E. Erikson, Chief Engr.
Rockford, Illinois

Systems Engineering Division
Pneumo Dynamics Corporation
4936 Fairmont Avenue
Bethesda 14, Maryland

Systems Technology, Inc.
ATTN: Mr. McRiver
1630 Centinala
Inglewood, California

Technical Information Division
Lawrence Radiation Laboratory
P.O.Box 808
Livermore, California

Temco Aircraft Corporation
Box 6191
Dallas 2, Texas

Sandia Corporation
Box 969
Livermore, California

Texaco Research and Development
Laboratories
ATTN: Mr. William Scarberry
P.O.Box 509
Beacon, New York

Thickel Chemical Corporation
Reaction Motors Division
ATTN: Mr. Goalwin
Denville, New Jersey

Thompson Ramo Woolridge, Inc.
TAPCO Group
ATTN: Mr. L. L. Aspelin
211 Hindry Avenue
Inglewood 1, California

Union Carbide Corporation
30 East 42nd Street
New York 17, New York

United Air Products
Engineering Department
Box 1035
Dayton 1, Ohio

University of California
Technical Information Division
ATTN: Clovis G. Craig
P.O.Box 808
Livermore, California

University of California at Los Angeles
Department of Chemistry
Los Angeles, California

University of Colorado
ATTN: Mr. Paul Barrick
Boulder, Colorado

University of Dayton
300 College Park Avenue
Dayton, Ohio

University of Utah
206 Mines Building
Salt Lake City, Utah

Vickers, Inc.
ATTN: Technical Information Service
Detroit 32, Michigan

University of Wichita
1845 Fairmount
Wichita 14, Kansas

University of Wisconsin
Naval Research Laboratory
Madison, Wisconsin

Wyandotte Chemical Corporation
Wyandotte, Michigan

Beech Aircraft Co.
Boulder Facility
P.O.Box 631
Boulder, Colorado

Bell Aircraft Corporation
Niagara Frontier Corporation
Niagara Falls 7, New York

Midwest Research Institute
ATTN: Mr. S. L. Levy
425 Volker Blvd.
Kansas City 10, Missouri

General Aniline and Film Corporation
ATTN: Mr. Hans Beller
435 Hudson Street
New York 14, New York

University of Denver
Denver Research Institute
ATTN: Dr. C. H. Prien
Denver, Colorado

University of Michigan
Aeronautical Engineering Laboratory
North Campus
Ann Arbor, Michigan

University of Minnesota
Rosement, Minnesota

University of Southern California
ATTN: Library
Los Angeles, California

Southern Research Institute
20000 Ninth Avenue
Birmingham, Alabama

TRG, Inc.
ATTN: Technical Library
2 Aerial Way
Syosset, Long Island, New York

Liquid Propellant Information Agency
The Johns Hopkins University
8621 Georgia Avenue
Silver Springs, Maryland

Englehard Industries, Inc.
ATTN: Mr. Tom Cushing
113 Astor Street
Newark, New Jersey

ASD, WPAFB, Ohio
ASNXRR
ASAPT (3 copies)
ASRCPR-2 (Mr. S. Zakanycz)
ASRMFP-2 (Mr. A. Fasano)
ASRCPT-1
ASROP

General Electric Company
Flight Propulsion Laboratory
Applied Research Operations Department
ATTN: Mr. J. B. Hancock, Mail Stop F-90
Cincinnati 15, Ohio

Lockheed California Corporation
Spacecraft Department (72-25) (Unit 40)
Post Office Box 551
ATTN: Mr. A.D. Schyner
Burbank, California

Air Reduction Co., Inc.
Central Research Labs
ATTN: Mr. G.A.Mead, II
200 Mountain Avenue
Murray Hill, New Jersey

Aeronautical and Missiles Division
Chance Vought Corporation
ATTN: Mr. Sal Love
P.O.Box 5907
Dallas 22, Texas

N-R-A Incorporated
ATTN: Melvin P. Ehrlich
38-15 Hunters Point Avenue
Long Island City 1, New York

Malaker Laboratories, Inc.
ATTN: Mr. Jerome B. Malaker
Sales Manager
West Main Street
High Bridge, New Jersey

Heliodyne Corporation
ATTN: Dr. Saul Feldman
2365 Westwood Boulevard
Los Angeles 64, California

Gardner Cryogenics Corporation
ATTN: Mr. W. E. Roebuck
Highstrown, New Jersey

U.S.Atomic Energy Commission
Office of Health and Safety
ATTN: Mr. R. B. Smith
Washington 25, D.C.

McDonald Aircraft Corporation
Technical Library
ATTN: Mr. Cole
P.O.Box 516, Municipal Airport
St. Louis 3, Missouri

Lawrence Radiation Laboratory
Technical Information Division
P.O.Box 808
Livermore, California

Hurcules Powder Company
Research Center
ATTN: Library
Wilmington, Delaware

Headquarters, USAF
DCS/Development
Pentagon, Rm 4A346
ATTN: Mr. Lorenzo
Washington 25, D.C.

General Motors Corporation
Defense Systems Division
ATTN: Dr. R.B.Costello
P.O.Drawer T
Santa Barbara, California

General Electric Company
Aircraft Division
ATTN: Library
P.O.Box 132
Cincinnati 15, Ohio

Electro-Optical Systems, Inc.
3016 East Foothill Boulevard
Pasadena, California

California Institute of Technology
Jet Propulsion Laboratory
ATTN: Mr. I.E.Newlan,
Technical Librarian
4800 Oak Grove Drive
Pasadena 3, California

AFFTC (FTRP/Mr.C.E.Lundblad)
Edwards AFB, California

Bell Aerospace Corporation
ATTN: Library
Wheatfield Plant
Buffalo 5, New York

Beech Aircraft Corporation
Boulder Facility
P.O.Box 631
Boulder, Colorado

Aerospace Corporation
ATTN: Mr.R.W.Vance, R.D.Long
Los Angeles, California

Stearns-Roger Manufacturing Company
ATTN: P.D.Fuller, J.N. McLagan
P.O.Box 5888
Denver 17, Colorado

Space-General Corporation
Space Systems Division
ATTN: S. G.Rumbold, Manager
Research Vehicle Programs
El Monte, California

Air Force Ballistics Systems Division
ATTN: Major G.J. Murphy
Requirement and Equipment Office
Los Angeles, California

Air Force Ballistics Systems Division
ATTN: Capt. P.O.Pearce
Atlas Program Office
Detachment 1, BSBRG
Norton AFB, California

University of South Carolina
ATTN: Chemical Engineering Department
Columbia, South Carolina

North Carolina State College
ATTN: Chemical Engineering Department
Raleigh, North Carolina

Space Technology Laboratories
ATTN: C.H.Reynales, M. Adelberg
Los Angeles, California

UNCLASSIFIED